Variational bounds on energy dissipation in incompressible flows. III. Convection

Charles R. Doering*
Center for Nonlinear Studies, MS-B258, Los Alamos National Laboratory, Los Alamos, New Mexico 87545

Peter Constantin†
Department of Mathematics, University of Chicago, Chicago, Illinois 60637

(Received 8 May 1995; revised manuscript received 16 January 1996)

Building on a method of analysis for the Navier-Stokes equations introduced by Hopf [Math. Ann. **117**, 764 (1941)], a variational principle for upper bounds on the largest possible time averaged convective heat flux is derived from the Boussinesq equations of motion. When supplied with appropriate test background fields satisfying a spectral constraint, reminiscent of an energy stability condition, the variational formulation produces rigorous upper bounds on the Nusselt number (Nu) as a function of the Rayleigh number (Ra). For the case of vertical heat convection between parallel plates in the absence of sidewalls, a simplified (but rigorous) formulation of the optimization problem yields the large Rayleigh number bound $\mathrm{Nu} \leqslant 0.167\ \mathrm{Ra}^{1/2} - 1$. Nonlinear Euler-Lagrange equations for the optimal background fields are also derived, which allow us to make contact with the upper bound theory of Howard [J. Fluid Mech. **17**, 405 (1963)] for statistically stationary flows. The structure of solutions of the Euler-Lagrange equations are elucidated from the geometry of the variational constraints, which sheds light on Busse's [J. Fluid Mech. **37**, 457 (1969)] asymptotic analysis of general solutions to Howard's Euler-Lagrange equations. The results of our analysis are discussed in the context of theory, recent experiments, and direct numerical simulations. [S1063-651X(96)06106-5]

PACS number(s): 47.27.Te, 03.40.Gc, 47.27.Cn, 47.27.Ak

I. INTRODUCTION

Conventional theoretical approaches to turbulence include approximate treatments ranging from the imposition of statistical assumptions and moment hierarchy truncations to the introduction of scaling hypotheses [1]. Rigorous analyses based solely on the equations of motion are typically less ambitious, hindered in part by the lack of a regularity proof for solutions of the three-dimensional Navier-Stokes equations [2]. In this paper we focus on a specific fundamental problem, the rate of heat transport in a layer of incompressible Newtonian fluid, with the goal of deriving quantitative rigorous results directly from the equations of motion *without any* statistical hypotheses, scaling assumptions, or closure approximations. Specifically, we establish a practical framework for estimating the viscous energy dissipation rate, and thus the convective heat flux, directly from the Boussinesq equations of motion without any additional regularity assumptions on the solutions. We do this by using the equations of motion to derive a variational principle for upper bounds on the time averaged heat transport rate, utilizing a decomposition that we refer to as the ''background field'' method. The basis of the principle is a decomposition of the flow field into a ''background'' and a ''fluctuation'' reminiscent of, but distinct from, the Reynolds decomposition into mean and fluctuating components familiar from statistical turbulence theory. Our approach is a development of Hopf's method for producing *a priori* estimates for solutions of the Navier-Stokes equations with inhomogeneous boundary conditions [3] and, as shown in the following sections, it appears more closely related to nonlinear hydrodynamic stability theory, i.e., the energy method [4], than to statistical turbulence theory. It applies equally to both laminar (stationary or time varying) and turbulent flows, yielding rigorous predictions free from uncontrolled approximations, and an interesting *a posteriori* relationship with statistical turbulence theory naturally follows from the analysis.

Consider an incompressible Newtonian fluid confined to the rectangular volume between rigid isothermal plates as illustrated in Fig. 1. A vertical temperature gradient of magnitude δT is imposed. In the usual nondimensional units the fluid's velocity vector field $\mathbf{u}(\mathbf{x},t)=(u_1,u_2,u_3)$ and temperature field $T(\mathbf{x},t)$ satisfy the Boussinesq equations

$$\frac{\partial \mathbf{u}}{\partial t} + \mathbf{u}\cdot\boldsymbol{\nabla}\mathbf{u} + \boldsymbol{\nabla} p = \sigma \Delta \mathbf{u} + \sigma\ \mathrm{Ra}\mathbf{k}T, \tag{1.1}$$

$$\boldsymbol{\nabla}\cdot\mathbf{u} = 0, \tag{1.2}$$

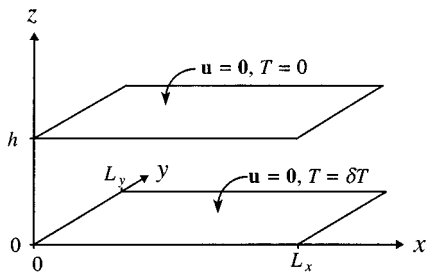

FIG. 1. Fluid is confined between parallel plates of dimension $L_x \times L_y$, separated by gap of height h in the z direction. Boundary conditions are periodic in the x and y directions and $T=\delta T$ for $z=0$, $T=0$ for $z=h$, and $\mathbf{u}=\mathbf{0}$ for $z=0$ and h.

*Address after 1 September 1996: Department of Mathematics, University of Michigan, Ann Arbor, Michigan 48109-1109. Electronic address: doering@cnls.lanl.gov

†Electronic address: const@zaphod.uchicago.edu

$$\frac{\partial T}{\partial t}+\mathbf{u}\cdot\boldsymbol{\nabla}T=\Delta T, \tag{1.3}$$

where $\sigma=\nu/\kappa$ is the Prandtl number (a ratio of material parameters, the kinematic viscosity ν and thermal diffusivity κ) and $\mathrm{Ra}=g\alpha\delta T h^3/\nu\kappa$ is the Rayleigh number (g is the acceleration of gravity, α is thermal expansion coefficient, δT is the temperature drop across the gap, and h is the gap width). Compressibility is neglected in all but the buoyancy force term, the last term in (1.1), and the pressure field $p(\mathbf{x},t)$ is determined by the divergence-free condition on $\mathbf{u}$. In (1.1), $\mathbf{k}$ is the unit vector in the z direction (the 3-direction). Lengths are measured in units of the gap width h and the boundary conditions in the dimensionless variables are no slip ($\mathbf{u}=\mathbf{0}$) on the $z=0$ and 1 planes, $T=0$ on top and $T=1$ on bottom, and periodic in the x and y directions, with periods L_x/h and L_y/h, respectively, for $\mathbf{u}$, T, and p. (From this point on, L_x and L_y will denote the dimensionless transverse lengths.) The initial temperature and velocity vector fields $\mathbf{u}(\mathbf{x},0)=\mathbf{u}_0(\mathbf{x})$ and $T(\mathbf{x},0)=T_0(\mathbf{x})$ are square integrable.

The conductive heat flux in the vertical direction is constant:

$$j=\int_0^{L_x}dx\int_0^{L_y}dy\int_0^1 dz\ \mathbf{k}\cdot[-\boldsymbol{\nabla}T(x,y,z,t)]=A, \tag{1.4}$$

where $A=L_xL_y$ is the cross-sectional area. The instantaneous convective heat flux is

$$J(t)=\int_0^{L_x}dx\int_0^{L_y}dy\int_0^1 dz\ u_3(x,y,z,t)T(x,y,z,t), \tag{1.5}$$

and the instantaneous rate of viscous energy dissipation in spatial dimension d (typically 2 or 3) is

$$\sigma\|\boldsymbol{\nabla}\mathbf{u}\|_2^2=\sigma\sum_{i,j=1}^{d}\left\|\frac{\partial u_i}{\partial x_j}\right\|_2^2, \tag{1.6}$$

where $\|f\|_2$ denotes the L^2 norm of a function $f(\mathbf{x})$:

$$\|f\|_2=\left(\int_0^{L_x}dx\int_0^{L_y}dy\int_0^1 dz|f(x,y,z)|^2\right)^{1/2}. \tag{1.7}$$

We are concerned with the time averaged convective heat flux

$$\langle J\rangle_t=\frac{1}{t}\int_0^t J(t')dt', \tag{1.8}$$

and the time averaged energy dissipation rate

$$\langle\sigma\|\boldsymbol{\nabla}\mathbf{u}\|_2^2\rangle_t=\frac{1}{t}\int_0^t\sigma\|\boldsymbol{\nabla}\mathbf{u}(\ ,t')\|_2^2dt'. \tag{1.9}$$

We define the Nusselt number as the ratio of the largest possible long time averaged total heat transport to the conductive heat transport

$$\mathrm{Nu}=\limsup_{t\to\infty}\frac{j+\langle J\rangle_t}{j}=1+\limsup_{t\to\infty}\frac{1}{A}\left\langle\int_0^{L_x}dx\int_0^{L_y}dy\int_0^1 dz\ u_3T\right\rangle_t, \tag{1.10}$$

where the lim sup notation refers to the limit supremum (the eventual least upper bound). The largest possible long time averaged energy dissipation rate per unit mass is denoted ε,

$$\varepsilon=\limsup_{t\to\infty}\frac{\langle\sigma\|\boldsymbol{\nabla}\mathbf{u}\|_2^2\rangle_t}{A}. \tag{1.11}$$

The connection between the heat flux and the energy dissipation is seen in the energy evolution equation derived from (1.1) by dotting with $\mathbf{u}$, integrating over space, and integrating by parts using the divergence free condition (1.2) and the boundary conditions:

$$\frac{d}{dt}\frac{1}{2}\|\mathbf{u}\|_2^2+\sigma\|\boldsymbol{\nabla}\mathbf{u}\|_2^2=\sigma\ \mathrm{Ra}J. \tag{1.12}$$

The kinetic energy is uniformly bounded for $t\in(0,\infty)$—this fact is a by-product of the analysis in this paper—so the average rate of viscous energy dissipation is proportional to the time averaged heat flux

$$\varepsilon=\sigma\ \mathrm{Ra}(\mathrm{Nu}-1). \tag{1.13}$$

Hence estimates of the average energy dissipation rate and bounds on the average flux are interchangeable, and in this application we will focus on the heat flux. The heat flux is also directly related to the mean square temperature gradient, as may be seen by multiplying the temperature evolution equation (1.3) by T and integrating appropriately:

$$\frac{d}{dt}\frac{1}{2}\|T\|_2^2+\|\boldsymbol{\nabla}T\|_2^2=A+J. \tag{1.14}$$

The temperature field remains uniformly bounded in L^2 (this fact may also be shown using some of the methods of analysis in this paper), so

$$\mathrm{Nu}=\limsup_{t\to\infty}\frac{\langle\|\boldsymbol{\nabla}T\|_2^2\rangle_t}{A}. \tag{1.15}$$

The ultimate goal is to produce a functional relationship of the form $\mathrm{Nu}(\mathrm{Ra},\sigma)$. Here we restrict ourselves to producing rigorous upper bounds on Nu in terms of Ra and σ by formulating a variational principle directly from the Boussinesq equations in which the fundamental constraint is identified with a stability condition in the sense of the energy method. The variational problem will be applied in two ways: (i) an upper bound is immediately produced by providing a ''test'' background field that satisfies the constraints and (ii) optimal background fields will be sought by mini-

mizing the bounds over the appropriately constrained set of test background fields. We derive Euler-Lagrange equations for the optimal fields, and in an intriguing correspondence we observe that they are of the same functional form as the Euler-Lagrange equations for the maximal heat flux in Howard's upper bound theory, which relies on an additional assumption on stationary statistics [5]. The general structure of the solutions of the Euler-Lagrange equations is determined by the functional geometry of the constraints, and at this level we find a further relationship with Busse's asymptotic analysis of Howard's theory [6]. For the separable geometry considered here, the simplest Euler-Lagrange equations, a nonlinear boundary value problem for ordinary differential equations, have solutions that correspond to the ''single wave number'' solutions of Howard's problem. The next level of complexity, a boundary value problem for two coupled sets of ordinary nonlinear differential equations, involves two wave numbers and so on. As will be seen, the transition from one type of solution to another involves a loss of stability.

The rest of this paper is organized as follows. The energy method is reviewed in Sec. II, focusing on the variational aspect of this approach to nonlinear stability. A variational principle for upper bounds on the time averaged flux is formulated in Sec. III and the nonlinear Euler-Lagrange equations for the optimal background fields are derived and discussed in Sec. IV. In Sec. V we use elementary estimates and asymptotics to produce explicit bounds (culminating with the large Rayleigh number bound $\mathrm{Nu}\leqslant 0.167\,\mathrm{Ra}^{1/2}-1$). In Sec. VI we analyze the optimal background problem to deduce an improved bound ($\mathrm{Nu}-1\leqslant 0.257\,\mathrm{Ra}^{3/8}$) when the Euler-Lagrange equations take on the simplest structure, which turns out to be the case for a bounded range of Ra ($\mathrm{Ra}\leqslant 23\,300$). Finally, in Sec. VII we compare these results with experiments, direct numerical simulations, and theories, pointing out directions for further development of this approach. For completeness, a brief synopsis of Howard's upper bound theory is provided in the Appendix.

This is the final article in a series of three following the introduction of this approach in an application to shear turbulence [7]. The first paper of the series developed the general approach for a boundary-driven shear layer [8]. Those results were compared with recent experiments [9] and have been further developed by others: Marchioro extended the method for application to time-dependent boundary conditions [10] and Gebhardt *et al.* reformulated the variational problem to refine the original analytical estimate [11]. The second paper in the series dealt with the problem of channel flow driven by a pressure gradient [12].

II. ENERGY STABILITY AND THE CALCULUS OF VARIATIONS

In this section we provide a short review of the elements of the energy method of nonlinear stability, which plays a major role in the subsequent analysis. Suppose $\mathbf{U}(\mathbf{x})$ and $\tau(\mathbf{x})$ are a stationary solution of the Boussinesq equations (1.1)–(1.3),

$$\mathbf{U}\cdot\boldsymbol{\nabla}\mathbf{U}+\boldsymbol{\nabla}P=\sigma\Delta\mathbf{U}+\sigma\ \mathrm{Ra}\mathbf{k}\tau, \tag{2.1}$$

$$\boldsymbol{\nabla}\cdot\mathbf{U}=0, \tag{2.2}$$

$$\mathbf{U}\cdot\boldsymbol{\nabla}\tau=\Delta\tau, \tag{2.3}$$

satisfying the velocity and temperature boundary conditions. Consider arbitrary perturbations (also known as fluctuations) $\mathbf{v}(\mathbf{x},t)$ and $\theta(\mathbf{x},t)$ of the stationary solution at hand, so that complete dynamic solutions $\mathbf{u}(\mathbf{x},t)$ and $T(\mathbf{x},t)$ are decomposed according to $\mathbf{u}(\mathbf{x},t)=\mathbf{U}(\mathbf{x})+\mathbf{v}(\mathbf{x},t)$ and $T=\tau(\mathbf{x})+\theta(\mathbf{x},t)$. The perturbations satisfy the evolution equations

$$\frac{\partial\mathbf{v}}{\partial t}+\mathbf{v}\cdot\boldsymbol{\nabla}\mathbf{v}+\mathbf{v}\cdot\boldsymbol{\nabla}\mathbf{U}+\mathbf{U}\cdot\boldsymbol{\nabla}\mathbf{v}+\boldsymbol{\nabla}p=\sigma\Delta\mathbf{v}+\sigma\ \mathrm{Ra}\mathbf{k}\theta, \tag{2.4}$$

$$\boldsymbol{\nabla}\cdot\mathbf{v}=0, \tag{2.5}$$

$$\frac{\partial\theta}{\partial t}+\mathbf{v}\cdot\boldsymbol{\nabla}\theta=\Delta\theta-\mathbf{U}\cdot\boldsymbol{\nabla}\theta-\mathbf{v}\cdot\boldsymbol{\nabla}\tau, \tag{2.6}$$

with the boundary conditions that $\mathbf{v}$ and θ both vanish on the top and bottom plates (periodic boundary conditions in the horizontal directions are taken throughout). Standard integrations by parts using the boundary conditions and (2.5) shows that the L^2 norms of the fluctuations evolve according to

$$\frac{d}{dt}\frac{1}{2}\|\mathbf{v}\|_2^2+\int\mathbf{v}\cdot\boldsymbol{\nabla}\mathbf{U}\cdot\mathbf{v}\,d\mathbf{x}=-\sigma\|\boldsymbol{\nabla}\mathbf{v}\|_2^2+\sigma\ \mathrm{Ra}\int v_3\theta\,d\mathbf{x}, \tag{2.7}$$

$$\frac{d}{dt}\frac{1}{2}\|\theta\|_2^2+\int\mathbf{v}\cdot\boldsymbol{\nabla}\tau\theta\,d\mathbf{x}=-|\boldsymbol{\nabla}\theta|_2^2. \tag{2.8}$$

The basic solution is said to be ''energy stable'' when the L^2 norms of the fluctuations decay monotonically.

Combining (2.7) and (2.8) appropriately, we find

$$\begin{aligned}\frac{d}{dt}\frac{1}{2}\left(\frac{1}{\sigma\ \mathrm{Ra}}\|\mathbf{v}\|_2^2+\|\theta\|_2^2\right)&\\ =-\int\left\{\frac{1}{\mathrm{Ra}}|\boldsymbol{\nabla}\mathbf{v}|^2+\frac{1}{\sigma\ \mathrm{Ra}}\mathbf{v}\cdot\boldsymbol{\nabla}\mathbf{U}\cdot\mathbf{v}+\mathbf{v}\cdot(\boldsymbol{\nabla}\tau-\mathbf{k})\theta\right.&\\ \left.+|\boldsymbol{\nabla}\theta|^2\right\}d\mathbf{x}.&\end{aligned} \tag{2.9}$$

Hence a sufficient condition for the L^2 norms of the fluctuations to decrease is that the right-hand side of (2.9) is always negative, i.e., that the quadratic functional

$$\begin{aligned}I_{\mathbf{U},\tau}\{\mathbf{v},\theta\}:=\int\left\{\frac{1}{\mathrm{Ra}}|\boldsymbol{\nabla}\mathbf{v}|^2+\frac{1}{\sigma\ \mathrm{Ra}}\mathbf{v}\cdot\boldsymbol{\nabla}\mathbf{U}\cdot\mathbf{v}\right.&\\ \left.+\mathbf{v}\cdot(\boldsymbol{\nabla}\tau-\mathbf{k})\theta+|\boldsymbol{\nabla}\theta|^2\right\}d\mathbf{x}&\end{aligned} \tag{2.10}$$

is positive for nonvanishing functions $\theta(\mathbf{x})$ and divergence-free vector fields $\mathbf{v}(\mathbf{x})$ satisfying the fluctuations' boundary conditions. When this is the case, the sum of the squares of the L^2 norms of the perturbations in (2.9) will decay exponentially with a minimum decay rate $\mu^{(0)}$, given by the solution of the minimization problem

$$\mu^{(0)} = \inf \left\{ \frac{I_{\mathbf{U},\tau}\{\mathbf{v},\theta\}}{\frac{1}{\sigma\ \mathrm{Ra}} \|\mathbf{v}\|_2^2 + \|\theta\|_2^2} \right\}, \tag{2.11}$$

where the infimum is taken over all temperature fields θ and divergence-free vector fields $\mathbf{v}$ satisfying the boundary conditions. Because the numerator and denominator are both quadratic in θ and $\mathbf{v}$, this may be rewritten

$$\mu^{(0)} = \inf I_{\mathbf{U},\tau}\{\mathbf{v},\theta\}, \tag{2.12}$$

where the minimization over $\mathbf{v}$ and θ is constrained by the normalization condition

$$1 = \frac{1}{\sigma\ \mathrm{Ra}} \|\mathbf{v}\|_2^2 + \|\theta\|_2^2. \tag{2.13}$$

Straightforward application of the calculus of variations shows that the temperature and velocity vector fields realizing the minimum exponential decay rate satisfy the Euler-Lagrange equations

$$\mu\mathbf{v} = -\sigma\Delta\mathbf{v} + \boldsymbol{\nabla} p + \tfrac{1}{2}(\boldsymbol{\nabla}\mathbf{U} + \boldsymbol{\nabla}\mathbf{U}^{\mathrm{tr}})\cdot\mathbf{v} + \tfrac{1}{2}\sigma\ \mathrm{Ra}(\boldsymbol{\nabla}\tau - \mathbf{k})\theta, \tag{2.14}$$

$$0 = \boldsymbol{\nabla}\cdot\mathbf{v}, \tag{2.15}$$

$$\mu\theta = -\Delta\theta + \tfrac{1}{2}\mathbf{v}\cdot(\boldsymbol{\nabla}\tau - \mathbf{k}), \tag{2.16}$$

where p is the Lagrange multiplier enforcing the divergence-free condition and tr means matrix transpose. Equations (2.14)–(2.16) constitute a self-adjoint spectral problem where the eigenvalue μ is the Lagrange multiplier enforcing the normalization constraint in (2.13). The minimum exponential decay rate $\mu^{(0)}$ is the lowest (ground state) eigenvalue of this problem and thus the nonlinear stability condition for the stationary solution $(\mathbf{U},\tau)$ may be expressed as the condition that this eigenvalue problem has a positive spectrum. Restated, energy stability considerations lead to a variational problem in (2.11) or (2.12), for which the Euler-Lagrange equations are the spectral problem in (2.14)–(2.16).

An increased Rayleigh number, appearing as it does as the prefactor of an indefinite operator in (2.14), generally leads to a decrease in nonlinear stability as measured by the positive magnitude of the lowest eigenvalue. Note that negative eigenvalues in the spectral problem for energy stability do *not* imply that the base solution is *not* a physically possible time asymptotic solution; it merely indicates the existence of initially nondecaying transients. It is necessary to look at the linearized eigenvalue problem to determine instability for small perturbations [13].

The purely conductive solution

$$\mathbf{U}(\mathbf{x}) = 0, \tag{2.17}$$

$$\tau(\mathbf{x}) = 1 - z \tag{2.18}$$

is a case in point. The energy stability eigenvalue problem for this solution is

$$\mu\mathbf{v} = -\sigma\Delta\mathbf{v} + \boldsymbol{\nabla} p - \sigma\ \mathrm{Ra}\mathbf{k}\theta, \tag{2.19}$$

$$0 = \boldsymbol{\nabla}\cdot\mathbf{v}, \tag{2.20}$$

$$\mu\theta = -\Delta\theta - v_3, \tag{2.21}$$

where we recognize the same eigenvalue problem as the *linearized* stability problem derived from Eqs. (1.1)–(1.3). The convection stability problem is a special case where the necessary and sufficient conditions for stability and instability match: $\mathrm{Ra}_c^{(\mathrm{nonlinear})} = \mathrm{Ra}_c^{(\mathrm{linear})} = \mathrm{Ra}_c > 1707$. This is also a special case where the Prandtl number drops out of the stability question, i.e., Ra_c does not depend on σ, but only on the aspect ratio of the convection cell (L_x, L_y).

For $\mathrm{Ra} < \mathrm{Ra}_c$, then, these considerations imply that the unique time asymptotic state of the system at hand is the pure conductive state in (2.17) and (2.18). Hence, in that case the long time averaged viscous energy dissipation rate vanishes ($\varepsilon = 0$) and the long time averaged heat transport is conductive (Nu=1). Both linear and nonlinear stability theory remain silent concerning ε and Nu beyond the critical Rayleigh number, but as will be shown in the next section, remarkably similar mathematical questions [i.e., the spectral analysis of a linear operator as in (2.14)–(2.16)] are relevant to the behavior of ε and Nu beyond the critical Rayleigh number, even into the turbulent regime.

III. ENERGY STABILITY AND ENERGY DISSIPATION

Long time limits of finite time averages need not exist even if finite time averages are bounded. Moreover, the long time averages in Eqs. (1.8) and (1.9) need not be unique: for even if the limit $t \to \infty$ did exist, it would generally depend on the initial conditions. Eventual bounds on the long time averages (the *limit suprema*) exist, nevertheless, and we may produce *a priori* estimates for those bounds directly from the equations of motion.

In this section we prove a variational principle for upper bounds on the largest possible long time averaged heat flux, expressing the upper estimate as an infimum over a constrained set of functions. As will be seen, the constraint is an effective (energy) stability constraint on flow and temperature fields. The variational bound is analogous to a Rayleigh-Ritz variational principle wherein upper estimates may be deduced without solving the entire minimization problem; just producing test functions satisfying the constraints is sufficient for that purpose.

To see how the bounds come about, we start by considering stationary solutions not to the equations of motion, but to a related set of partial differential equations. Let $\mathbf{U}(\mathbf{x})$ and $\tau(\mathbf{x})$ satisfy

$$\mathbf{U}\cdot\boldsymbol{\nabla}\mathbf{U} + \boldsymbol{\nabla} P = \sigma\ \mathrm{Ra}\mathbf{k}\tau, \tag{3.1}$$

$$\boldsymbol{\nabla}\cdot\mathbf{U} = 0, \tag{3.2}$$

$$\mathbf{U}\cdot\boldsymbol{\nabla}\tau = 0, \tag{3.3}$$

along with the boundary conditions ($\mathbf{U}=0$ for $z=0$ and 1, $\tau=1$ for $z=0$, $\tau=0$ for $z=1$, and everything periodic in the horizontal directions). These are an ''inviscid'' version of the stationary Boussinesq equations, characterized by the absence of the Laplacian terms. Many solutions to these equations exist and an entire class of explicit solutions will be produced below. We refer to a solution $(\mathbf{U},\tau)$ to Eqs. (3.1)–(3.3) as ''background'' flow and temperature fields.

Consider arbitrary perturbations (fluctuations) $\mathbf{v}(\mathbf{x},t)$ and $\theta(\mathbf{x},t)$ of the background fields, so that complete solutions $\mathbf{u}(\mathbf{x},t)$ and $T(\mathbf{x},t)$ are decomposed according to $\mathbf{u}(\mathbf{x},t)=\mathbf{U}(\mathbf{x})+\mathbf{v}(\mathbf{x},t)$ and $T=\tau(\mathbf{x})+\theta(\mathbf{x},t)$. The perturbations satisfy

$$\frac{\partial \mathbf{v}}{\partial t}+\mathbf{v}\cdot\boldsymbol{\nabla}\mathbf{v}+\mathbf{v}\cdot\boldsymbol{\nabla}\mathbf{U}+\mathbf{U}\cdot\boldsymbol{\nabla}\mathbf{v}+\boldsymbol{\nabla}p=\sigma\Delta\mathbf{v}+\sigma\Delta\mathbf{U}+\sigma\ \mathrm{Ra}\mathbf{k}\theta, \tag{3.4}$$

$$\boldsymbol{\nabla}\cdot\mathbf{v}=0, \tag{3.5}$$

$$\frac{\partial \theta}{\partial t}+\mathbf{v}\cdot\boldsymbol{\nabla}\theta=\Delta\theta+\Delta\tau-\mathbf{U}\cdot\boldsymbol{\nabla}\theta-\mathbf{v}\cdot\boldsymbol{\nabla}\tau, \tag{3.6}$$

with the boundary conditions that $\mathbf{v}$ and θ both vanish on the top and bottom plates (same boundary conditions as for the energy stability analysis). The L^2 norms of these fluctuations evolve according to

$$\frac{d}{dt}\frac{1}{2}\|\mathbf{v}\|_2^2+\int \mathbf{v}\cdot\boldsymbol{\nabla}\mathbf{U}\cdot\mathbf{v}\,d\mathbf{x}=-\sigma\|\boldsymbol{\nabla}\mathbf{v}\|_2^2-\sigma\int \boldsymbol{\nabla}\mathbf{v}:\boldsymbol{\nabla}\mathbf{U}\,d\mathbf{x}+\sigma\ \mathrm{Ra}\int v_3\theta\,d\mathbf{x}, \tag{3.7}$$

$$\frac{d}{dt}\frac{1}{2}\|\theta\|_2^2+\int \mathbf{v}\cdot\boldsymbol{\nabla}\tau\theta\,d\mathbf{x}=-\|\boldsymbol{\nabla}\theta\|_2^2-\int \boldsymbol{\nabla}\theta\cdot\boldsymbol{\nabla}\tau\,d\mathbf{x}. \tag{3.8}$$

Note that norms of the gradients of the full solutions satisfy

$$\|\boldsymbol{\nabla}\mathbf{u}\|_2^2=\|\boldsymbol{\nabla}\mathbf{U}\|_2^2+2\sigma\int \boldsymbol{\nabla}\mathbf{v}:\boldsymbol{\nabla}\mathbf{U}\,d\mathbf{x}+\|\boldsymbol{\nabla}\mathbf{u}\|_2^2, \tag{3.9}$$

$$\|T\|_2^2=\|\tau\|_2^2+2\int \boldsymbol{\nabla}\theta\cdot\boldsymbol{\nabla}\tau\,d\mathbf{x}+\|\theta\|_2^2, \tag{3.10}$$

which may be used to eliminate the cross terms (involving $\boldsymbol{\nabla}\mathbf{v}:\boldsymbol{\nabla}\mathbf{U}$ and $\boldsymbol{\nabla}\theta\cdot\boldsymbol{\nabla}\tau$) on the right-hand sides of (3.7) and (3.8):

$$\frac{d}{dt}\frac{1}{2}\|\mathbf{v}\|_2^2+\int \mathbf{v}\cdot\boldsymbol{\nabla}\mathbf{U}\cdot\mathbf{v}\,d\mathbf{x}=-\frac{\sigma}{2}\|\boldsymbol{\nabla}\mathbf{v}\|_2^2-\frac{\sigma}{2}\|\mathbf{u}\|_2^2+\frac{\sigma}{2}\|\boldsymbol{\nabla}\mathbf{U}\|_2^2+\sigma\ \mathrm{Ra}\int v_3\theta\,d\mathbf{x}, \tag{3.11}$$

$$\frac{d}{dt}\frac{1}{2}\|\theta\|_2^2+\int \mathbf{v}\cdot\boldsymbol{\nabla}\tau\theta\,d\mathbf{x}=-\tfrac{1}{2}\|\boldsymbol{\nabla}\theta\|_2^2-\tfrac{1}{2}\|\boldsymbol{\nabla}T\|_2^2+\tfrac{1}{2}\|\boldsymbol{\nabla}\tau\|_2^2. \tag{3.12}$$

Combining (3.11) and (3.12) appropriately, we find

$$\frac{d}{dt}\frac{1}{2}\left(\frac{1}{\sigma\ \mathrm{Ra}}\|\mathbf{v}\|_2^2+\|\theta\|_2^2\right)+\frac{1}{2\ \mathrm{Ra}}\|\boldsymbol{\nabla}\mathbf{u}\|_2^2+\tfrac{1}{2}\|\boldsymbol{\nabla}T\|_2^2=\frac{1}{2\ \mathrm{Ra}}\|\boldsymbol{\nabla}\mathbf{U}\|_2^2+\tfrac{1}{2}\|\boldsymbol{\nabla}\tau\|_2^2-\int\left\{\frac{1}{2\ \mathrm{Ra}}|\boldsymbol{\nabla}\mathbf{v}|^2+\frac{1}{\sigma\ \mathrm{Ra}}\mathbf{v}\cdot\boldsymbol{\nabla}\mathbf{U}\cdot\mathbf{v}+\mathbf{v}\cdot(\boldsymbol{\nabla}\tau-\mathbf{k})\theta+\tfrac{1}{2}|\boldsymbol{\nabla}\theta|^2\right\}d\mathbf{x}. \tag{3.13}$$

The time average of (3.13) yields

$$\frac{1}{t}\left(\frac{1}{\sigma\ \mathrm{Ra}}\|\mathbf{v}(\cdot,t)\|_2^2-\frac{1}{\sigma\ \mathrm{Ra}}\|\mathbf{v}(\cdot,0)\|_2^2+\|\theta(\cdot,t)\|_2^2-\|\theta(\cdot,0)\|_2^2\right)+\frac{1}{\mathrm{Ra}}\langle\|\boldsymbol{\nabla}\mathbf{u}\|_2^2\rangle_t+\langle\|\boldsymbol{\nabla}T\|_2^2\rangle_t=\frac{1}{\mathrm{Ra}}\|\boldsymbol{\nabla}\mathbf{U}\|_2^2+\|\boldsymbol{\nabla}\tau\|_2^2+2\left\langle-\int\left\{\frac{1}{2\ \mathrm{Ra}}|\boldsymbol{\nabla}\mathbf{v}|^2+\frac{1}{\sigma\ \mathrm{Ra}}\mathbf{v}\cdot\boldsymbol{\nabla}\mathbf{U}\cdot\mathbf{v}+\mathbf{v}\cdot(\boldsymbol{\nabla}\tau-\mathbf{k})\theta+\tfrac{1}{2}|\boldsymbol{\nabla}\theta|^2\right\}d\mathbf{x}\right\rangle_t. \tag{3.14}$$

Because $\mathbf{u}$, $\mathbf{v}$, T, and θ stay bounded in L^2 (we do not prove this fact explicitly, but it follows from some of methods developed here; see the analogous argument in Ref. [7], for example) we may take the long time limit supremum of (3.14) combined with the time averaged versions of (1.12) and (1.14) to obtain

$$A+2\limsup_{t\to\infty}\langle J\rangle_t=\frac{1}{\mathrm{Ra}}\|\boldsymbol{\nabla}\mathbf{U}\|_2^2+\|\boldsymbol{\nabla}\tau\|_2^2+\limsup_{t\to\infty}\langle-2H_{\mathbf{U},\tau}\{\mathbf{v},\theta\}\rangle_t, \tag{3.15}$$

where the quadratic functional $H_{\mathbf{U},\tau}\{\mathbf{v},\theta\}$ of $\mathbf{v}$ and θ is defined by

$$H_{\mathbf{U},\tau}\{\mathbf{v},\theta\}:=\int\left\{\frac{1}{2\ \mathrm{Ra}}|\boldsymbol{\nabla}\mathbf{v}|^2+\frac{1}{\sigma\ \mathrm{Ra}}\mathbf{v}\cdot\boldsymbol{\nabla}\mathbf{U}\cdot\mathbf{v}+\mathbf{v}\cdot(\boldsymbol{\nabla}\tau-\mathbf{k})\theta+\tfrac{1}{2}|\boldsymbol{\nabla}\theta|^2\right\}d\mathbf{x}. \tag{3.16}$$

The argument now proceeds by noting that *if* $H_{\mathbf{U},\tau}\{\mathbf{v},\theta\}\geqslant 0$, i.e., if it is a non-negative quadratic form for divergence-free vector fields $\mathbf{v}$ and functions θ satisfying the fluctuations' boundary conditions, *then* the background fields provide an upper limit on the energy dissipation rate and convective heat transport:

$$A+2\limsup_{t\to\infty}\langle J\rangle_t\leqslant\frac{1}{\mathrm{Ra}}\|\boldsymbol{\nabla}\mathbf{U}\|_2^2+\|\boldsymbol{\nabla}\tau\|_2^2. \tag{3.17}$$

The conditions on $\mathbf{U}$ and τ imposed by the constraint $H_{\mathbf{U},\tau} \geqslant 0$ are remarkably analogous to the energy stability criterion $I_{\mathbf{U},\tau} > 0$ for stationary solutions of the Boussinesq equations: $H_{\mathbf{U},\tau}$ and $I_{\mathbf{U},\tau}$ differ only by coefficients of 2 in their positive definite terms in the integrand. Unraveling (3.17), we deduce the heat transport bound

$$\mathrm{Nu} \leqslant \frac{1}{2} + \frac{1}{2A}\left(\frac{1}{\mathrm{Ra}}\,\|\boldsymbol{\nabla}\mathbf{U}\|_2^2 + \|\boldsymbol{\nabla}\tau\|_2^2\right) \tag{3.18}$$

provided that the fields $\mathbf{U}$ and τ (a) are solutions of the ''inviscid'' equations (3.1)–(3.3) satisfying the boundary conditions for the stationary Boussinesq problem and (b) are ''stable'' in the sense that $H_{\mathbf{U},\tau}$ is non-negative.

We will refer to the apparent marginal energy stability condition on acceptable background flow and temperature fields as the *spectral constraint*. Exploiting this analogy further, we will also refer to background fields $(\mathbf{U},\tau)$ with $H_{\mathbf{U},\tau} > 0$ as *stable* background fields and those with $H_{\mathbf{U},\tau} \geqslant 0$ as *marginally stable* background fields. Indeed, in direct analogy to the energy stability problem, whether or not $H_{\mathbf{U},\tau}$ is non-negative is determined by the sign of $\lambda^{(0)}$, given by the solution of the minimization problem

$$\lambda^{(0)} = \inf\left\{\frac{H_{\mathbf{U},\tau}\{\mathbf{v},\theta\}}{\dfrac{1}{\sigma\ \mathrm{Ra}}\,\|\mathbf{v}\|_2^2 + \|\theta\|_2^2}\right\}. \tag{3.19}$$

The infimum is to be taken over all temperature fields θ and divergence-free vector fields $\mathbf{v}$ satisfying the fluctuations' boundary conditions. Further, because the numerator and denominator are both quadratic in θ and $\mathbf{v}$, this may be rewritten

$$\lambda^{(0)} = \inf H_{\mathbf{U},\tau}\{\mathbf{v},\theta\}, \tag{3.20}$$

where the minimization over $\mathbf{v}$ and θ is additionally constrained by the normalization condition

$$1 = \frac{1}{\sigma\ \mathrm{Ra}}\,\|\mathbf{v}\|_2^2 + \|\theta\|_2^2. \tag{3.21}$$

The temperature and velocity vector fields realizing the minimum in (3.19), or (3.20) and (3.21) satisfy the Euler-Lagrange equations

$$\lambda\mathbf{v} = -\sigma\Delta\mathbf{v} + \boldsymbol{\nabla}p + (\boldsymbol{\nabla}\mathbf{U} + \boldsymbol{\nabla}\mathbf{U}^{\mathrm{tr}})\cdot\mathbf{v} + \sigma\ \mathrm{Ra}(\boldsymbol{\nabla}\tau - \mathbf{k})\,\theta, \tag{3.22}$$

$$0 = \boldsymbol{\nabla}\cdot\mathbf{v}, \tag{3.23}$$

$$\lambda\,\theta = -\Delta\,\theta + \mathbf{v}\cdot(\boldsymbol{\nabla}\tau - \mathbf{k}), \tag{3.24}$$

where p is the Lagrange multiplier enforcing the condition $\boldsymbol{\nabla}\cdot\mathbf{v} = 0$ and tr means matrix transpose. Equations (3.22)–(3.24) constitute a self-adjoint spectral problem, the eigenvalue λ being the Lagrange multiplier enforcing the normalization constraint in (3.21). The extremum $\lambda^{(0)}$ is the lowest (ground state) eigenvalue of this problem and thus the spectral constraint on the background fields $(\mathbf{U},\tau)$ is the condition that this eigenvalue problem has a non-negative spectrum, i.e., $\lambda^{(0)} \geqslant 0$.

Restated, time averaged energy evolution considerations lead to the bounds in (3.17) and (3.18) subject to the constraint on $H_{\mathbf{U},\tau}$, leading in turn to the variational problem in (3.19), or (3.20)–(3.21), for which the Euler-Lagrange equations are the spectral problem in (3.22)–(3.24). The first challenge is to produce appropriate background fields and verify the spectral constraint, which will be done explicitly in Sec. V. Ultimately the goal is to produce the *best* background fields, which will themselves be the solution of a constrained minimization problem where the spectral constraint, itself the result of a minimization problem, is imposed. The next section is concerned with developing a version of the ''ultimate'' constrained variational problem and to deriving the associated Euler-Lagrange equations for optimal background fields. Afterward, in Sec. VI, the optimal background fields will be analyzed to produce improved bounds over a restricted range of Ra.

IV. VARIATIONS ON A VARIATION: OPTIMAL BACKGROUND FIELDS

Restrict attention to the class of background fields consisting of horizontally stratified temperature profiles and plane parallel shear flows:

$$\mathbf{U}(\mathbf{x}) = \mathbf{i}U(z), \tag{4.1}$$

$$\tau(\mathbf{x}) = \tau(z), \tag{4.2}$$

where $U(0) = 0 = U(1)$, $\tau(0) = 1$, and $\tau(1) = 0$. It is easy to see that any such functions satisfy the background field equations (3.1)–(3.3). Only the shear rate and thermal gradients enter into the problem from this point on, so we introduce the functions

$$\phi(z) = \frac{dU(z)}{dz}, \tag{4.3}$$

$$\psi(z) = 1 + \frac{d\tau(z)}{dz}, \tag{4.4}$$

which are in one-to-one correspondence with the background profiles $U(z)$ and $\tau(z)$ when they are constrained to have mean zero:

$$\int_0^1 \phi(z)\,dz = 0, \tag{4.5}$$

$$\int_0^1 \psi(z)\,dz = 0. \tag{4.6}$$

Then the upper bound problem can be cast in the form of a variational problem. In the preceding section we proved the following.

Theorem. For every solution of Eqs. (1.1)–(1.3) with the prescribed boundary conditions,

$$\mathrm{Nu} \leqslant 1 + \inf\left\{\frac{1}{2}\,\frac{1}{\mathrm{Ra}}\int_0^1 \phi(z)^2\,dz + \frac{1}{2}\int_0^1 \psi(z)^2\,dz\right\}, \tag{4.7}$$

where the minimization is performed over mean-zero functions ϕ and ψ constrained by the spectral condition that

$$0 \leqslant H_{\phi,\psi}\{\mathbf{v},\theta\} = \int \left\{ \frac{1}{2\,\mathrm{Ra}} |\boldsymbol{\nabla}\mathbf{v}|^2 + \frac{1}{\sigma\,\mathrm{Ra}}\,\phi(z) v_1 v_3 + [\psi(z)-2] v_3\theta + \tfrac{1}{2}\,|\boldsymbol{\nabla}\theta|^2 \right\} d\mathbf{x}, \quad (4.8)$$

where $H_{\phi,\psi}\{\mathbf{v},\theta\}$ is defined for divergence-free vector fields $\mathbf{v}(\mathbf{x})$ and temperature fields θ satisfying the fluctuations' boundary conditions.

The spectral constraint is equivalent to the non-negativity of the lowest (''ground state'') eigenvalue $\lambda^{(0)}$ of the self-adjoint problem

$$\lambda v_1 = -\sigma\Delta v_1 + \frac{\partial p}{\partial x} + \phi(z) v_3, \quad (4.9)$$

$$\lambda v_2 = -\sigma\Delta v_2 + \frac{\partial p}{\partial y}, \quad (4.10)$$

$$\lambda v_3 = -\sigma\Delta v_3 + \frac{\partial p}{\partial z} + \phi(z) v_1 + \sigma\,\mathrm{Ra}[\psi(z)-2]\theta, \quad (4.11)$$

$$0 = \frac{\partial v_1}{\partial x} + \frac{\partial v_2}{\partial y} + \frac{\partial v_3}{\partial z}, \quad (4.12)$$

$$\lambda\theta = -\Delta\theta + [\psi(z)-2] v_3, \quad (4.13)$$

with boundary conditions $\mathbf{v}=0$ and $\theta=0$ for $z=0$ and 1 and everything periodic in x and y. In the above, p is the Lagrange multiplier enforcing incompressibility and λ is the Lagrange multiplier enforcing the natural normalization for the eigenfunctions,

$$1 = \frac{1}{\sigma\,\mathrm{Ra}} \|v\|_2^2 + \|\theta\|_2^2. \quad (4.14)$$

In the following we will use the notation $\lambda^{(0)} = \lambda^{(0)}\{\phi,\psi\}$ to explicitly display the functional dependence of the ground state eigenvalue on the background profile functions ϕ and ψ.

The one-sided nature of the spectral constraint ($\lambda^{(0)}\{\phi,\psi\} \geqslant 0$) makes the variational problem for the extremum temperature and flow profiles appear nonstandard. However, a simple observation allows us to transform the constraint into an equality ($\lambda^{(0)}\{\phi,\psi\}=0$), making way for the application of the usual method of Lagrange multipliers to implement it. The key observation is that the set of background profiles $[\phi(z),\psi(z)]$ satisfying $\lambda^{(0)}\{\phi,\psi\} \geqslant 0$ is *convex* in the Hilbert space of pairs of mean zero, square integrable functions on [0,1]. This means that if (ϕ_1,ψ_1) and (ϕ_2,ψ_2) each satisfy the spectral constraint, then for $0 \leqslant t \leqslant 1$ the convex combination $[t\phi_1+(1-t)\phi_2, t\psi_1+(1-t)\psi_2]$ also satisfies the spectral constraint. This is seen by writing $\lambda^{(0)}\{\phi_1,\psi_1\}$ and $\lambda^{(0)}\{\phi_2,\psi_2\}$ in the variational forms

$$\lambda^{(0)}\{\phi_1,\psi_1\} = \inf \int \left\{ \frac{1}{2\,\mathrm{Ra}} |\boldsymbol{\nabla}\mathbf{v}|^2 + \frac{1}{\sigma\,\mathrm{Ra}}\,\phi_1(z) v_1 v_3 + [\psi_1(z)-2] v_3\theta + \tfrac{1}{2}\,|\boldsymbol{\nabla}\theta|^2 \right\} d\mathbf{x}, \quad (4.15)$$

$$\lambda^{(0)}\{\phi_2,\psi_2\} = \inf \int \left\{ \frac{1}{2\,\mathrm{Ra}} |\boldsymbol{\nabla}\mathbf{v}|^2 + \frac{1}{\sigma\,\mathrm{Ra}}\,\phi_2(z) v_1 v_3 + [\psi_2(z)-2] v_3\theta + \tfrac{1}{2}\,|\boldsymbol{\nabla}\phi|^2 \right\} d\mathbf{x}, \quad (4.16)$$

where the infima are taken over the set of normalized [according to (4.14)] divergence-free $\mathbf{v}$'s and θ's satisfying the fluctuations' boundary conditions. When both $\lambda^{(0)}\{\phi_1,\psi_1\}$ and $\lambda^{(0)}\{\phi_2,\psi_2\}$ are non-negative, then the right-hand sides above are non-negative for *any* appropriate $\mathbf{v}$ and θ. Hence for any such appropriate $\mathbf{v}$ and θ, the convex combination of the functionals is non-negative,

$$0 \leqslant \int \left\{ \frac{1}{2\,\mathrm{Ra}} |\boldsymbol{\nabla}\mathbf{v}|^2 + \frac{1}{\sigma\,\mathrm{Ra}} [t\phi_1+(1-t)\phi_2] v_1 v_3 + [t\psi_1+(1-t)\psi_2-2] v_3\theta + \tfrac{1}{2}\,|\boldsymbol{\nabla}\theta|^2 \right\} d\mathbf{x} = H_{t\phi_1+(1-t)\phi_2,\, t\psi_1+(1-t)\psi_2}, \quad (4.17)$$

and taking the infimum over $\mathbf{v}$ and θ we deduce

$$0 \leqslant \lambda^{(0)}\{t\phi_1+(1-t)\phi_2, t\psi_1+(1-t)\psi_2\}. \quad (4.18)$$

This convexity property implies that the minimization in (4.7) is realized in one of two ways. The absolute minimum possible value of the Nusselt number (Nu=1) is realized at the origin of the space of profiles, i.e., $(\phi,\psi)=(0,0)$, and this will be the solution of the variational problem if the pair (0,0) satisfies the spectral constraint; see Fig. 2(a). A sufficient condition for this is stability of the pure conduction state, the state of affairs at low Rayleigh number. At high Ra, the origin is no longer contained in the convex set of spectrally constrained background functions and the bound on Nu-1 is precisely the square of the distance from the origin to the convex set, where we utilize the L^2 norm

$$\|(\phi,\psi)\| = \left(\frac{1}{\mathrm{Ra}} \int_0^1 \phi(z)^2 dz + \int_0^1 \psi(z)^2 dz \right)^{1/2}. \quad (4.19)$$

The distance to a nonempty convex set *not* containing the origin is *uniquely* realized by a point on the *boundary* of the set as illustrated in Fig. 2(b). (The existence of the solution is guaranteed by the nonemptiness of the convex set, which we shall establish in Sec. V.) We conclude that when the origin does not satisfy the spectral constraint, the minimization problem is solved by a background profile just marginally satisfying it, i.e., the optimal background profile pair is *on* the isospectral surface $\lambda^{(0)}\{\phi,\psi\}=0$.

Now we are in a position to apply conventional constrained variational calculus. For Ra high enough so that $(\phi,\psi)=(0,0)$ does not satisfy the spectral constraint, the Euler-Lagrange equations for the optimal background fields are

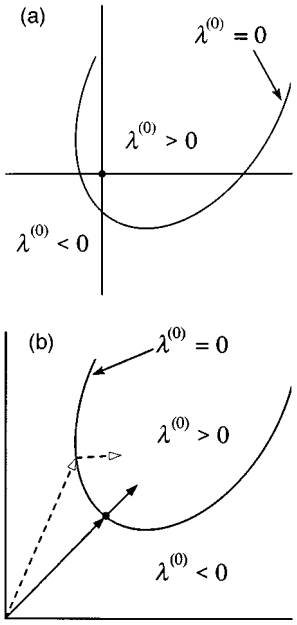

FIG. 2. Illustration of the functional convexity property enjoyed by the background fields (ϕ,ψ) in (a two-dimensional slice of) the function space of pairs of mean-zero functions on the unit interval. The origin is the optimal point when it is contained in the convex set, as in (a), and the unique optimal point (dot) occurs on the boundary when the origin is not contained in the set, as in (b). In (b) the normal vectors to the isospectral surface of marginally stable profiles are shown at two points. Typically (dashed) the normal is not aligned with vector from the origin, while the optimal (solid) occurs when the vector from the origin is parallel to the normal vector.

$$0 = \frac{\delta}{\delta(\phi,\psi)} \left\{ \tfrac{1}{2}\|(\phi,\psi)\|^2 + \alpha \int_0^1 \phi(z)\,dz + \beta \int_0^1 \psi(z)\,dz + \gamma \lambda^{(0)}\{\phi,\psi\} \right\}, \tag{4.20}$$

where α, β, and γ are Lagrange multipliers. Explicitly, these equations are

$$0 = \phi(z) + \alpha + \gamma \frac{\delta \lambda^{(0)}}{\delta \phi(z)}, \tag{4.21}$$

$$0 = \psi(z) + \beta + \gamma \frac{\delta \lambda^{(0)}}{\delta \psi(z)}, \tag{4.22}$$

where the variational derivatives of the ground state eigenvalue are evaluated by the usual method of regular spectral perturbation theory:

$$\frac{\delta \lambda^{(0)}}{\delta \phi(z)} = 2 \int_0^{L_x} dx \int_0^{L_y} dy\; v_1^{(0)}(x,y,z) v_3^{(0)}(x,y,z), \tag{4.23}$$

$$\frac{\delta \lambda^{(0)}}{\delta \psi(z)} = 2 \int_0^{L_x} dx \int_0^{L_y} dy\; v_3^{(0)}(x,y,z)\,\theta^{(0)}(x,y,z). \tag{4.24}$$

In the above, $\mathbf{v}^{(0)}$ and $\theta^{(0)}$ are the ground state eigenfunctions of (4.9)–(4.13) normalized according to (4.14). The Lagrange multipliers α and β are chosen to enforce the mean-zero constraint on ϕ and ψ so (4.21) and (4.22) become

$$\phi(z) = 2\gamma \left(\int_0^{L_x} dx \int_0^{L_y} dy\; v_1^{(0)}(x,y,z) v_3^{(0)}(x,y,z) - \int_0^1 dz' \int_0^{L_x} dx \int_0^{L_y} dy\; v_1^{(0)}(x,y,z') v_3^{(0)}(x,y,z') \right) \tag{4.25}$$

and

$$\psi(z) = 2\gamma \left(\int_0^{L_x} dx \int_0^{L_y} dy\; v_3^{(0)}(x,y,z)\,\theta^{(0)}(x,y,z) - \int_0^1 dz' \int_0^{L_x} dx \int_0^{L_y} dy\; v_3^{(0)}(x,y,z')\,\theta^{(0)}(x,y,z') \right), \tag{4.26}$$

where γ is the remaining Lagrange multiplier used to enforce the marginal stability constraint.

The equations to be solved, then, are the ground state equations (4.9)–(4.13) closed by (4.25) and (4.26); this is a nonlinear and nonlocal elliptic boundary value problem in which the Lagrange multiplier γ is to be adjusted so that $\lambda^{(0)}$ vanishes. The optimal flow and temperature profiles are subsequently reconstructed from the resulting ground state eigenfunctions $\mathbf{v}^{(0)}$ and $\theta^{(0)}$ via (4.25) and (4.26).

The Euler-Lagrange equations (4.25) and (4.26) may also be derived from a geometric argument in a picture that gives us some insight into the nature of the solutions of the optimization problem. Assume for the moment that the marginally stable isospectral surface where $\lambda^{(0)}=0$ is smooth in the sense that there exists a unique, one-dimensional normal vector at and near the optimal point. Referring to the sketch of the geometry in Fig. 2(b), it is clear that the optimal solution is that point in the Hilbert space enjoying the property that the vector connecting the origin to the isospectral surface $\lambda^{(0)}=0$ is aligned with the normal vector to the isospectral surface. The normal vector is precisely the functional derivative $[\delta\lambda^{(0)}/\delta\phi(z), \delta\lambda^{(0)}/\delta\psi(z)]$ projected onto the space of pairs of mean-zero functions. Let γ be the proportionality constant between the vector $[\phi(z),\psi(z)]$—from the origin to the optimal point—and the normal vector. The Euler-Lagrange equations are then (4.25) and (4.26). This geometric viewpoint also makes it clear that when the origin is not contained in the set with $\lambda^{(0)}>0$, then the Lagrange multiplier γ is necessarily positive (the vectors are parallel and not antiparallel).

In view of the horizontal translation invariance of the eigenvalue problem in (4.9)–(4.13), the equations may be separated by the Fourier transform in the horizontal directions and this suggests a strategy for solving the Euler-Lagrange equations. We define the horizontally Fourier transformed variables

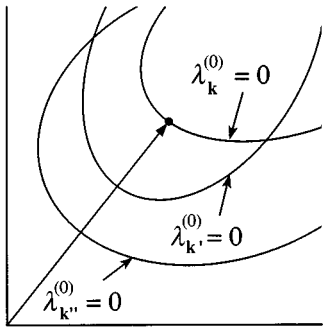

FIG. 3. Isospectral surfaces in (a two-dimensional slice of) the space of background functions, for three different wave numbers. The convex set over which the variation takes place is the intersection of the convex sets for each wave number. The optimal profile is on one of the isospectral surfaces, furthest from the origin.

$$\begin{pmatrix} u_{\mathbf{k}}(z) \\ v_{\mathbf{k}}(z) \\ w_{\mathbf{k}}(z) \\ q_{\mathbf{k}}(z) \\ \zeta_{\mathbf{k}}(z) \end{pmatrix} = \frac{1}{L_x L_y} \int_0^{L_x} dx\, e^{-ik_1 x} \int_0^{L_y} dy\, e^{-ik_2 y} \begin{pmatrix} v_1(x,y,z) \\ v_2(x,y,z) \\ v_3(x,y,z) \\ p(x,y,z) \\ \theta(x,y,z) \end{pmatrix}, \tag{4.27}$$

where $\mathbf{k}=(k_1,k_2)=(2\pi n_1/L_1, 2\pi n_2/L_2)$ and (n_1,n_2) are pairs of integers. Then $\partial/\partial x \to ik_1$ and $\partial/\partial y \to ik_2$ and, using the notation $k^2=|\mathbf{k}|^2=k_1^2+k_2^2$ and $D=\partial/\partial z$, the eigenvalue problem becomes

$$\lambda_{\mathbf{k}} u_{\mathbf{k}} = \sigma(-D^2+k^2)u_{\mathbf{k}} + ik_1 q_{\mathbf{k}} + \phi(z) w_{\mathbf{k}}, \tag{4.28}$$

$$\lambda_{\mathbf{k}} v_{\mathbf{k}} = \sigma(-D^2+k^2)v_{\mathbf{k}} + ik_2 q_{\mathbf{k}}, \tag{4.29}$$

$$\lambda_{\mathbf{k}} w_{\mathbf{k}} = \sigma(-D^2+k^2)w_{\mathbf{k}} + Dq_{\mathbf{k}} + \phi'(z)u_{\mathbf{k}} + \sigma\,\mathrm{Ra}[\psi(z)-2]\zeta_{\mathbf{k}}, \tag{4.30}$$

$$0 = ik_1 u_{\mathbf{k}} + ik_2 v_{\mathbf{k}} + Dw_{\mathbf{k}}, \tag{4.31}$$

$$\lambda_{\mathbf{k}} \zeta_{\mathbf{k}} = (-D^2+k^2)\zeta_{\mathbf{k}} + [\psi(z)-2]w_{\mathbf{k}}, \tag{4.32}$$

with boundary conditions $u_{\mathbf{k}}(z)$, $v_{\mathbf{k}}(z)$, $w_{\mathbf{k}}(z)$, and $\zeta_{\mathbf{k}}(z)$ vanishing at $z=0$ and 1. The ground state eigenvalue will be denoted $\lambda_{\mathbf{k}}^{(0)}=\lambda_{\mathbf{k}}^{(0)}\{\phi,\psi\}$.

As illustrated in Fig. 3, for each wave vector $\mathbf{k}$ there is a convex set of stable background profiles characterized by $\lambda_{\mathbf{k}}^{(0)}\{\phi,\psi\}>0$, with an isospectral surface of marginally stable profiles given by $\lambda_{\mathbf{k}}^{(0)}\{\phi,\psi\}=0$. The set over which the minimization takes place is the intersection of the stable sets for all the wave numbers:

$$\{(\phi,\psi)|\lambda^{(0)}\{\phi,\psi\}\geqslant 0\} = \cap_{\mathbf{k}}\{(\phi,\psi)|\lambda_{\mathbf{k}}^{(0)}\{\phi,\psi\}\geqslant 0\}. \tag{4.33}$$

When the overall marginally stable isospectral surface $\lambda^{(0)}\{\phi,\psi\}=0$ is smooth, then the surface is realized by one of the single wave number isospectral surfaces (modulo nongeneric tangencies of isospectral surfaces). The optimal point $[\phi_{\mathbf{k}}(z),\psi_{\mathbf{k}}(z)]$ on the $\mathbf{k}$th isospectral surface is also characterized by the property that it is parallel to (the projection onto mean-zero functions of) the functional derivative $[\delta\lambda_{\mathbf{k}}^{(0)}/\delta\phi(z), \delta\lambda_{\mathbf{k}}^{(0)}/\delta\psi(z)]$. That is, it is the solution to (4.28)–(4.32) closed by the relations

$$\phi_{\mathbf{k}}(z) = \gamma_{\mathbf{k}}\Big(u_{\mathbf{k}}^{(0)}(z)^* w_{\mathbf{k}}^{(0)}(z) + u_{\mathbf{k}}^{(0)}(z) w_{\mathbf{k}}^{(0)}(z)^* - \int_0^1 \{u_{\mathbf{k}}^{(0)}(z')^* w_{\mathbf{k}}^{(0)}(z') + u_{\mathbf{k}}^{(0)}(z') w_{\mathbf{k}}^{(0)}(z')^*\} dz' \Big) \tag{4.34}$$

and

$$\psi_{\mathbf{k}}(z) = \gamma_{\mathbf{k}}\Big(\zeta_{\mathbf{k}}^{(0)}(z)^* w_{\mathbf{k}}^{(0)}(z) + \zeta_{\mathbf{k}}^{(0)}(z) w_{\mathbf{k}}^{(0)}(z)^* - \int_0^1 \{\zeta_{\mathbf{k}}^{(0)}(z')^* w_{\mathbf{k}}^{(0)}(z') + \zeta_{\mathbf{k}}^{(0)}(z') w_{\mathbf{k}}^{(0)}(z')^*\} dz' \Big). \tag{4.35}$$

Expressions (4.34) and (4.35) inserted into (4.28)–(4.32) result in ordinary differential equations, a nonlinear boundary value problem where the Lagrange multiplier $\gamma_{\mathbf{k}}$ is to be adjusted to enforce the $\lambda_{\mathbf{k}}^{(0)}=0$ constraint. The true optimal background profile is that which is furthest from the origin—it must be furthest for otherwise it would be exterior to the stable region of some other wave number—so the strategy is to solve the problem for each individual $\mathbf{k}$ and then choose the one with the largest value of $\|(\phi,\psi)\|$. The minimization scheme proposed for each $\mathbf{k}$ has been shown to be consistent and the entire process has been carried out for a model problem [14], and to illustrate how this process works in practice we will apply the formalism to derive explicit upper bounds for the heat transport in Sec. V. Furthermore, it is straightforward to implement this procedure (minimize for each $\mathbf{k}$ and then maximize over $\mathbf{k}$) numerically and, as will be described in full detail elsewhere [15], the $\mathbf{k}$ by $\mathbf{k}$ strategy is successful, at least for a limited range of Rayleigh numbers.

There is a crucial point about this solution process that must be recognized: whenever a candidate background field is derived as the result of the min-max process described above it must be stable for *all* wave numbers in order to be the true solution. The single-$\mathbf{k}$ isospectral surfaces move around as Ra varies, and what can go wrong with the procedure outlined above is that the optimal profile may become degenerate. The onset of degeneracy means that the optimal has ground state eigenvalue zero for distinct wave numbers, signaling an intersection of the single wave number isospectral surfaces. This indicates that the optimal for nearby values of Ra will *not* generally be on a smooth portion of the overall marginally stable isospectral surface, as illustrated in Fig. 4. It is apparent that the optimal is then no longer characterized by the criteria given above relating the normal to

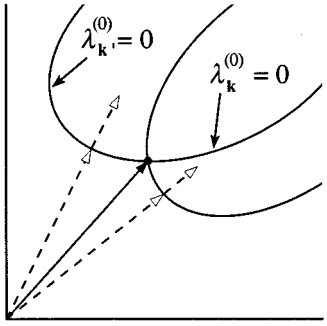

FIG. 4. If the ground state at the optimal is not unique, then each of the degenerate ground states gives rise to a normal and in general they need not coincide. In that case the isospectral surface is not smooth at the optimal and the min-max procedure is invalid.

the vector from the origin: indeed, there is not a unique normal vector at the optimal point and the optimal is further from the origin than the maximum distance to the single-**k** isospectral surfaces individually.

The problem may still be interpreted geometrically. Referring to Fig. 5 for the case of doubly degenerate optimal background fields, the question is how to characterize the closest point to the origin on the intersection of two marginally stable isospectral surfaces. The codimension-2 set where the two codimension-1 isospectral surfaces intersect does not have a normal vector, but instead a normal 2-form (associated with the linear subspace spanned by the two simultaneous normal vectors corresponding to the two isospectral surfaces). The generalization of the geometric criterion for the optimal is that the vector connecting the origin to the optimal point must be spanned by (i.e., a linear combination of) the normal vectors making up the 2-form at the optimal point.

Let $\mathbf{k}_1$ and $\mathbf{k}_2$ be the wave vectors of the optimal background field, with $\lambda_1^{(0)}\{\phi,\psi\}$ and $\lambda_2^{(0)}\{\phi,\psi\}$ the corresponding ground state eigenvalue functionals. Then the Euler-Lagrange equations expressing this criterion are

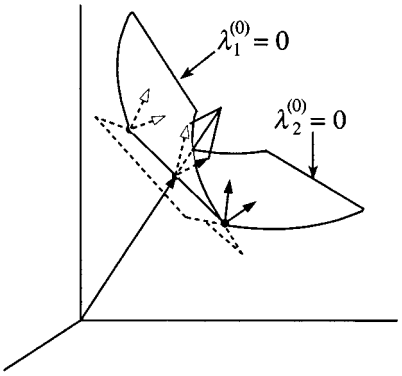

FIG. 5. Isospectral surfaces in (a three-dimensional slice of) the space of background functions, for two different wave numbers. This is the picture when the ground state of the optimal background fields is doubly degenerate. The optimal point occurs when the vector from the origin lies in the plane spanned by the two normals along the codimension-2 surface.

$$\phi(z)=\gamma_1\left(\frac{\delta\lambda_1^{(0)}}{\delta\phi(z)}-\int_0^1\frac{\delta\lambda_1^{(0)}}{\delta\phi(z')}\,dz'\right)+\gamma_2\left(\frac{\delta\lambda_2^{(0)}}{\delta\phi(z)}-\int_0^1\frac{\delta\lambda_2^{(0)}}{\delta\phi(z')}\,dz'\right) \tag{4.36}$$

and

$$\psi(z)=\gamma_1\left(\frac{\delta\lambda_1^{(0)}}{\delta\psi(z)}-\int_0^1\frac{\delta\lambda_1^{(0)}}{\delta\psi(z')}\,dz'\right)+\gamma_2\left(\frac{\delta\lambda_2^{(0)}}{\delta\psi(z)}-\int_0^1\frac{\delta\lambda_2^{(0)}}{\delta\psi(z')}\,dz'\right), \tag{4.37}$$

where

$$\frac{\delta\lambda_i^{(0)}}{\delta\phi(z)}=u_i^{(0)}(z)^*w_i^{(0)}(z)+u_i^{(0)}(z)w_i^{(0)}(z)^* \tag{4.38}$$

and

$$\frac{\delta\lambda_i^{(0)}}{\delta\psi(z)}=\zeta_i^{(0)}(z)^*w_i^{(0)}(z)+\zeta_i^{(0)}(z)w_i^{(0)}(z)^*. \tag{4.39}$$

Expressions (4.36) and (4.37) are then to be inserted into (4.28)–(4.32) for $\mathbf{k}_1$ and $\mathbf{k}_2$ simultaneously, which constitute a closed system to be solved while adjusting the Lagrange multipliers γ_1 and γ_2 so that both $\lambda_1^{(0)}$ and $\lambda_2^{(0)}$ vanish.

When the optimal background fields are doubly degenerate they lie on a set of codimension 2 in the space of background functions and the Euler-Lagrange equations are a system of two coupled nonlinear ordinary differential boundary value problems.

This process may be generalized: when the optimal background fields are N-fold degenerate they lie on a set of codimension N in the space of background functions and the Euler-Lagrange equations are a system of N coupled nonlinear ordinary differential boundary value problems. The coupling occurs through the simultaneous appearance of contributions of N wave vectors in the relationship between the optimal profiles and the ground state eigenfunctions according the generalization of the formulas above,

$$\phi(z)=\sum_{i=1}^N\gamma_i\left(\frac{\delta\lambda_i^{(0)}}{\delta\phi(z)}-\int_0^1\frac{\delta\lambda_i^{(0)}}{\delta\phi(z')}\,dz'\right), \tag{4.40}$$

$$\psi(z)=\sum_{i=1}^N\gamma_i\left(\frac{\delta\lambda_i^{(0)}}{\delta\psi(z)}-\int_0^1\frac{\delta\lambda_i^{(0)}}{\delta\psi(z')}\,dz'\right). \tag{4.41}$$

Solving the N equations for $\mathbf{k}_1,\ldots,\mathbf{k}_N$ simultaneously, each of the N Lagrange multipliers γ_i is to be adjusted so that $\lambda_i^{(0)}=0$, $i=1,\ldots,N$, placing the point on the marginally stable isospectral surface.

It is worthwhile noting that the solutions of all these classes of problems are indeed solutions of the originally posited Euler-Lagrange equations in (4.25) and (4.26). In the partial differential equation formulation, the nonlocal nonlinearity allows for separation via Fourier transformation in the horizontal variables, but the separation may be to into a varying number of components depending on the coupling of different wave vectors in the expression for the optimal

background fields. This is what corresponds to the hierarchy of classes of solutions, to our identification of the degeneracy condition, and to the presence of higher-dimensional ''creases'' in the marginal isospectral surface. In light of these correspondences we may interchangeably refer to the optimal fields as lying on codimension-N hypersurfaces, as being background fields with an N-fold degenerate ground state, or as comprising N wave vector solutions of the Euler-Lagrange equations.

For the case of vanishing background flow ($\phi \equiv 0$ from the beginning), the Euler-Lagrange equations derived here for the optimal background temperature profile are of the same functional form as the Euler-Lagrange equations in Howard's [5] upper bound theory for turbulent convection. In that work the variational problem is to determine the maximum heat transport constrained by the power balance derived from the Boussinesq equations supplemented with the hypothesis of ''statistical stationarity,'' i.e., the assumption that horizontal spatial averages are time independent [5,16]. This correspondence in the forms of the resulting Euler-Lagrange equations is surprising at least because the present analysis involves no statistical hypothesis. We note, however, that the actual differential equations to be solved are not precisely the same due to different appearances of Lagrange multipliers, which must be adjusted to satisfy different constraints. We have not been able to identify a direct connection between the fundamental variational problems posed by Howard and ourselves: only this quantitative relationship at the level of the optimal background profile appears to be the common feature of the two optimization problems. But this correspondence is enough to allow for a quantitative comparison of the results of the two approaches, and the relationship between the heat transport bounds in Howard's theory and the bounds derived by the method developed here will be discussed further in Sec. VI and the Appendix, where a rigorous connection between the two is established.

In his original paper [5] Howard recognized the variety of solutions to the Euler-Lagrange equations that potentially exist, but he concentrated on deriving estimates under the further presumption that the maximizing fields were of the single wave number variety. Busse's asymptotic analysis of Howard's Euler-Lagrange equations [6] implied that the maximizing fields are single wave number solutions only for a bounded range in Ra and that in a sequence of discrete transitions the N wave number solutions realize the maxima where N increases without bound as Ra increases. If this same phenomenon occurs in the background flow formulation, then the picture that emerges is one where the ground state of the optimal profile necessarily becomes increasingly degenerate as Ra increases. That is, the optimal profile becomes increasingly marginal in the sense that it is marginally stable for an ever increasing number of wave numbers. We will return to this point further in the discussion in the concluding section, but now we turn to the problem of producing explicit bounds, establishing first that the convex set of stable background flow profiles is not empty.

V. EXPLICIT BOUNDS NEGLECTING INCOMPRESSIBILITY

Rigorous analytical bounds on the heat transport may easily be obtained from the variational formulation by restricting the trial background fields further. Although the bounds obtained in this section will not be optimal, the process of deriving them will be useful for guiding the analysis of optimal solutions in Sec. VI. Moreover, the existence of a stable background profile (optimal or not) guarantees that the convex set of stable profiles is nonempty and thus that a unique optimal background field exists.

Choose the background flow field to be zero [$U(z) = 0 \Leftrightarrow \phi(z) = 0$], so the upper bound is

$$\mathrm{Nu} \leqslant 1 + \frac{1}{2}\int_0^1 \psi(z)^2 dz, \tag{5.1}$$

for functions $\psi(z)$ satisfying

$$\int_0^1 \psi(z)\,dz = 0, \tag{5.2}$$

and the spectral constraint

$$0 \leqslant H_\psi\{\mathbf{v},\theta\} = \int \left\{ \frac{1}{2\,\mathrm{Ra}} |\boldsymbol{\nabla}\mathbf{v}|^2 + [\psi(z) - 2] v_3 \theta + \tfrac{1}{2}|\nabla\theta|^2 \right\} d\mathbf{x}, \tag{5.3}$$

defined for divergence-free vector fields $\mathbf{v}(\mathbf{x})$ and temperature fields θ satisfying the fluctuations' boundary conditions. Note that the Prandtl number drops out of the picture in this restricted formulation.

The conduction profile corresponding to $\psi = 0$ is an acceptable trial function only for small enough Ra where the indefinite cross term ($\sim v_3\theta$) in H_ψ is dominated by the positive definite first and last terms ($\sim|\mathbf{v}|^2$ and $|\boldsymbol{\nabla}\theta|^2$). For high Ra the temperature profile must be adjusted to enforce the spectral constraint. If $\psi(z) = 2$, then (5.3) holds, but (5.2) is violated. The task is to satisfy (5.2) and (5.3) simultaneously, which is accomplished by choosing ψ so that $\psi \approx 2$ on most of the interval [0,1] with departures near the boundaries at $z = 0$ and 1, where v_3 and θ are forced to zero by their boundary conditions.

What works is a background temperature profile $\tau(z)$ of the form

$$\tau(z) = \begin{cases} 1 - \left(\dfrac{1}{\delta} - 1\right) z, & 0 \leqslant z \leqslant \delta \\ z, & \delta \leqslant z \leqslant 1 - \delta \\ \left(\dfrac{1}{\delta} - 1\right)(1 - z), & 1 - \delta \leqslant z \leqslant 1, \end{cases} \tag{5.4}$$

as illustrated in Fig. 6. The parameter δ ($0 < \delta \leqslant \frac{1}{2}$) will be referred to as the ''boundary layer thickness'' and the associated ψ function is

$$\psi(z) = \tau'(z) + 1 = \begin{cases} 2 - \dfrac{1}{\delta}, & 0 \leqslant z \leqslant \delta \\ 2, & \delta \leqslant z \leqslant 1 - \delta \\ 2 - \dfrac{1}{\delta}, & 1 - \delta \leqslant z \leqslant 1. \end{cases} \tag{5.5}$$

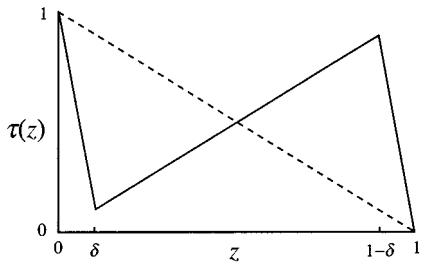

FIG. 6. Trial background temperature profile $\tau(z)$, as given in (5.4). The parameter δ is referred to as the boundary layer thickness. The dashed line is the temperature profile in the pure conduction state.

As we will now establish, the boundary layer thickness in this profile may be adjusted so that the spectral constraint is satisfied.

Rather than solving the eigenvalue problem corresponding to (5.3) in order to verify the spectral constraint, we may perform the analysis directly in terms of the quadratic form $H_\psi\{\mathbf{v},\theta\}$. The cross term in H_ψ is estimated in terms of the first and last terms as

$$\begin{aligned}\left|\int\ [\psi(z)-2]v_3\theta\ dx\right| &= \frac{1}{\delta}\left|\int_0^{L_x}dx\int_0^{L_y}dy\int_0^{\delta}dz\ v_3\theta\right.\\ &\quad\left.+\int_0^{L_x}dx\int_0^{L_y}dy\int_{1-\delta}^{1}dz\ v_3\theta\right|\\ &\leqslant \frac{1}{\delta}\left(\left|\int_0^{L_x}dx\int_0^{L_y}dy\int_0^{\delta}dz\ v_3\theta\right|\right.\\ &\quad\left.+\left|\int_0^{L_x}dx\int_0^{L_y}dy\int_{1-\delta}^{1}dz\ v_3\theta\right|\right).\end{aligned} \tag{5.6}$$

Consider the first term in the set of large parentheses in (5.6). Because v_3 and θ both vanish at $z=0$, the fundamental theorem of calculus ensures that

$$\begin{aligned}&\left|\int_0^{L_x}dx\int_0^{L_y}dy\int_0^{\delta}dz\ v_3\theta\right|\\ &\quad=\left|\int_0^{L_x}dx\int_0^{L_y}dy\int_0^{\delta}dz\left(\int_0^{z}dz'\ \frac{\partial v_3(x,y,z')}{\partial z'}\right)\right.\\ &\qquad\left.\times\left(\int_0^{z}dz''\ \frac{\partial\theta(x,y,z'')}{\partial z''}\right)\right|.\end{aligned} \tag{5.7}$$

Elementary application of the Schwarz inequality implies

$$\left|\int_0^{z}dz'\ \frac{\partial v_3(x,y,z')}{\partial z'}\right|\leqslant\sqrt{z}\left[\int_0^{z}dz'\left(\frac{\partial v_3}{\partial z'}\right)^2\right]^{1/2}, \tag{5.8}$$

$$\left|\int_0^{z}dz''\ \frac{\partial\theta(x,y,z'')}{\partial z''}\right|\leqslant\sqrt{z}\left[\int_0^{z}dz''\left(\frac{\partial\theta}{\partial z''}\right)^2\right]^{1/2}. \tag{5.9}$$

Combining (5.8) and (5.9) with (5.7) we observe that

$$\begin{aligned}&\left|\int_0^{L_x}dx\int_0^{L_y}dy\int_0^{\delta}dz\ v_3\theta\right|\\ &\quad\leqslant\left|\int_0^{L_x}dx\int_0^{L_y}dy\int_0^{\delta}dz\ z\right.\\ &\qquad\left.\times\left[\int_0^{\delta}dz'\left(\frac{\partial v_3}{\partial z'}\right)^2\right]^{1/2}\left[\int_0^{\delta}dz''\left(\frac{\partial\theta}{\partial z''}\right)^2\right]^{1/2}\right|,\end{aligned} \tag{5.10}$$

where we have also extended the upper limit in the z' and z'' integrations all the way to δ. The z integral in (5.10) may be performed, and applying the Schwarz inequality to the x and y integrals as well, we find

$$\begin{aligned}&\left|\int_0^{L_x}dx\int_0^{L_y}dy\int_0^{\delta}dz\ v_3\theta\right|\\ &\quad\leqslant\frac{\delta^2}{2}\left[\int_0^{L_x}dx\int_0^{L_y}dy\int_0^{\delta}dz'\left(\frac{\partial v_3}{\partial z'}\right)^2\right]^{1/2}\\ &\qquad\times\left[\int_0^{L_x}dx\int_0^{L_y}dy\int_0^{\delta}dz''\left(\frac{\partial\theta}{\partial z''}\right)^2\right]^{1/2}.\end{aligned} \tag{5.11}$$

A similar expression holds for the other end of the interval near $z=1$. Putting together (5.11) and the corresponding result near $z=1$ with the aid of the inequality $2ab\leqslant ca^2+b^2/c$, where the positive parameter c is free for the moment, we deduce

$$\begin{aligned}&\left|\int\ [\psi(z)-2]v_3\theta\ d\mathbf{x}\right|\\ &\qquad\leqslant\frac{1}{\delta}\times\frac{\delta^2}{2}\times\frac{1}{2}\left(c\left\|\frac{\partial v_3}{\partial z}\right\|_2^2+c^{-1}\left\|\frac{\partial\theta}{\partial z}\right\|_2^2\right).\end{aligned} \tag{5.12}$$

The incompressibility condition can now be used to sharpen the estimate. Note first that by multiplying $0=\boldsymbol{\nabla}\cdot\mathbf{v}$ by $\partial v_3/\partial z$ we have

$$0=\left(\frac{\partial v_3}{\partial z}\right)^2+\frac{\partial v_3}{\partial z}\frac{\partial v_1}{\partial x}+\frac{\partial v_3}{\partial z}\frac{\partial v_2}{\partial y}. \tag{5.13}$$

Integrating (5.13) over the volume and integrating by parts on the right-hand side to exchange the derivatives, we find

$$0=\left\|\frac{\partial v_3}{\partial z}\right\|_2^2+\int\left\{\frac{\partial v_1}{\partial z}\frac{\partial v_3}{\partial x}+\frac{\partial v_2}{\partial z}\frac{\partial v_3}{\partial y}\right\}d\mathbf{x}. \tag{5.14}$$

Likewise, squaring $\partial v_3/\partial z=-(\partial v_1/\partial x+\partial v_2/\partial y)$, integrating, integrating by parts on the cross term, and rearranging yields

$$0=\left\|\frac{\partial v_3}{\partial z}\right\|_2^2-\left\|\frac{\partial v_1}{\partial x}\right\|_2^2-\left\|\frac{\partial v_2}{\partial y}\right\|_2^2-2\int\ \frac{\partial v_1}{\partial y}\frac{\partial v_2}{\partial x}\,d\mathbf{x}. \tag{5.15}$$

Now, adding twice (5.14) and once (5.15) to $\|\boldsymbol{\nabla}\mathbf{v}\|_2^2$, we deduce

$$\|\nabla \mathbf{v}\|_2^2 = \left\| \frac{\partial v_1}{\partial y} - \frac{\partial v_2}{\partial x} \right\|_2^2 + \left\| \frac{\partial v_1}{\partial z} + \frac{\partial v_3}{\partial x} \right\|_2^2 + \left\| \frac{\partial v_2}{\partial z} + \frac{\partial v_3}{\partial y} \right\|_2^2 + 4 \left\| \frac{\partial v_3}{\partial z} \right\|_2^2 \geq 4 \left\| \frac{\partial v_3}{\partial z} \right\|_2^2. \tag{5.16}$$

Thus (5.12) may be rewritten

$$\left| \int [\psi(z) - 2] v_3 \theta \, d\mathbf{x} \right| \leq \frac{\delta}{4} \left(\frac{c}{4} \|\nabla \mathbf{v}\|_2^2 + \frac{1}{c} \|\nabla \theta\|_2^2 \right). \tag{5.17}$$

The functional $H_\psi\{\mathbf{v}, \theta\}$ may now be bounded below:

$$H_\psi\{\mathbf{v}, \theta\} \geq \left(\frac{1}{2\,\mathrm{Ra}} - \frac{\delta c}{16} \right) \|\nabla \mathbf{v}\|_2^2 + \left(\frac{1}{2} - \frac{\delta}{4c} \right) \|\nabla \theta\|_2^2. \tag{5.18}$$

First choose $c = \delta/2$ so that

$$H_\psi\{\mathbf{v}, \theta\} \geq \left(\frac{1}{2\,\mathrm{Ra}} - \frac{\delta^2}{32} \right) \|\nabla \mathbf{v}\|_2^2. \tag{5.19}$$

To ensure the spectral constraint, then, we choose the boundary layer thickness δ according to

$$\delta = \frac{4}{\sqrt{\mathrm{Ra}}}. \tag{5.20}$$

We may now evaluate the upper bound on the convective heat transport:

$$\mathrm{Nu} \leq 1 + \frac{1}{2} \int_0^1 \psi(z)^2 dz = 1 + \frac{1}{\delta} - 2 = \frac{1}{4} \sqrt{\mathrm{Ra}} - 1, \tag{5.21}$$

valid for $\mathrm{Ra} \geq 64$ so that $\delta \leq \frac{1}{2}$.

We may improve this estimate slightly, reducing the prefactor, although leaving the exponent alone, by utilizing the variational technology for the optimal profile. That is, we can solve a simpler related problem that is not completely optimal, but still produces a rigorous result. The calculation proceeds in two steps: first, the variational problem is reformulated with the spectral constraint replaced by a new constraint, stronger than the original but simpler in form, and, second, the optimal profile subject to the new constraint is found exactly. This exercise illustrates the implementation of much of the variational machinery and will be useful for giving insight into the nature of the ultimate optimal solution discussed in Sec. VI.

For functions $v_3(z), \theta(z)$ vanishing at $z = 0$ and 1 define the functional

$$K_\psi\{v_3, \theta\} = \int_0^1 \left\{ \frac{4}{2\,\mathrm{Ra}} \left| \frac{\partial v_3}{\partial z} \right|^2 + [\psi(z) - 2] v_3 \theta + \frac{1}{2} \left| \frac{\partial \theta}{\partial z} \right|^2 \right\} dz. \tag{5.22}$$

Then using (5.16), the functional defining the spectral constraint is seen to satisfy

$$H_\psi\{\mathbf{v}, \theta\} = \int \left\{ \frac{1}{2\,\mathrm{Ra}} |\nabla \mathbf{v}|^2 + [\psi(z) - 2] v_3 \theta + \tfrac{1}{2} |\nabla \theta|^2 \right\} d\mathbf{x} \geq \int \left[\int_0^1 \left\{ \frac{4}{2\,\mathrm{Ra}} \left| \frac{\partial v_3}{\partial z} \right|^2 + [\psi(z) - 2] v_3 \theta + \frac{1}{2} \left| \frac{\partial \theta}{\partial z} \right|^2 \right\} dz \right] dx \, dy = \int K_\psi\{v_3(x,y,\cdot), \theta(x,y,\cdot)\} dx \, dy. \tag{5.23}$$

Hence if K_ψ (defined for functions on $z \in [0,1]$) is nonnegative definite, then so is H_ψ (defined on θ and divergence free $\mathbf{v}$ satisfying the boundary conditions under consideration). This implies that the result of the minimization problem over $\psi(z)$ constrained by $K_\psi \geq 0$ is an upper bound on the result of the minimization problem over $\psi(z)$ constrained by $H_\psi \geq 0$. We have thus derived an alternative, albeit weaker, variational bound on the heat transport:

$$\mathrm{Nu} \leq 1 + \frac{1}{2} \int_0^1 \psi(z)^2 dz, \tag{5.24}$$

for functions $\psi(z)$ satisfying

$$\int_0^1 \psi(z) dz = 0, \tag{5.25}$$

and the spectral constraint

$$0 \leq \int_0^1 \left\{ \frac{1}{2} (Dw)^2 + \left(\frac{\mathrm{Ra}}{4} \right)^{1/2} [\psi(z) - 2] w \theta + \frac{1}{2} (D\theta)^2 \right\} dz, \tag{5.26}$$

where $D = d/dz$ and the test functions $w(z)$ and $\theta(z)$ vanish at $z = 0$ and 1. [The integration variable v_3 in the functional K_ψ in (5.22) has been replaced by $w = (\sqrt{4/\mathrm{Ra}}) v_3$ in (5.26).] This variational bound is necessarily higher than the original formulation because the new spectral constraint is stronger, but the minimization can be carried out exactly, which, as will be shown below, leads to an improved prefactor as compared to the nonoptimal result in (5.21).

The spectral condition for this minimization refers to the sign of the lowest eigenvalue of the self-adjoint problem

$$\lambda w = -D^2 w + \left(\frac{\mathrm{Ra}}{4} \right)^{1/2} [\psi(z) - 2] \theta, \tag{5.27}$$

$$\lambda \theta = -D^2 \theta + \left(\frac{\mathrm{Ra}}{4} \right)^{1/2} [\psi(z) - 2] w. \tag{5.28}$$

This eigenvalue problem may be ''diagonalized'' by going to new dependent variables

$$f(z) = \frac{1}{\sqrt{2}} [w(z) + \theta(z)], \tag{5.29}$$

$$g(z)=\frac{1}{\sqrt{2}}\,[w(z)-\theta(z)], \tag{5.30}$$

whereupon (5.27) and (5.28) transform to

$$\lambda f=-D^2f+\left(\frac{\mathrm{Ra}}{4}\right)^{1/2}[\psi(z)-2]f, \tag{5.31}$$

$$\lambda g=-D^2g-\left(\frac{\mathrm{Ra}}{4}\right)^{1/2}[\psi(z)-2]g \tag{5.32}$$

for real functions $f(z)$ and $g(z)$, $z\in[0,1]$, with Dirichlet boundary conditions. Some care must be taken at this point: the ground state eigenvalue of (5.27) and (5.28) is the lesser of the ground state eigenvalues for the independent problems (5.31) and (5.32). Equivalently, non-negativity of $K_\psi\{v_3,\theta\}$ is the same as non-negativity of *both*

$$K^+_\psi\{f\}=\int_0^1\left\{\frac{1}{2}\,(Df\,)^2+\frac{1}{2}\left(\frac{\mathrm{Ra}}{4}\right)^{1/2}[\psi(z)-2]f^2\right\}dz \tag{5.33}$$

and

$$K^-_\psi\{g\}=\int_0^1\left\{\frac{1}{2}\,(Dg)^2-\frac{1}{2}\left(\frac{\mathrm{Ra}}{4}\right)^{1/2}[\psi(z)-2]g^2\right\}dz. \tag{5.34}$$

Therefore the set of appropriate mean zero ψ over which we need to minimize is the intersection $\{\psi|K^+_\psi\geqslant 0$ and $K^-_\psi\geqslant 0\}=\{\psi|K^+_\psi\geqslant 0\}\cap\{\psi|K^-_\psi\geqslant 0\}$. Note that among mean-zero functions $\psi(z)$, $\{\psi|K^-_\psi\geqslant 0\}$ contains $\psi\equiv 0$ for every value of Ra. This suggests what we will now do: vary over the set $\{\psi|K^+_\psi=0\}$ and afterward verify that the ensuing extremal function is in $\{\psi|K^-_\psi\geqslant 0\}$. This guarantees that the solution we produce is indeed the true minimum over the intersection and is roughly analogous to the max-min procedure described in Sec. IV for the full optimal problem.

So consider the eigenvalue problem

$$\lambda f=-D^2f+\left(\frac{\mathrm{Ra}}{4}\right)^{1/2}[\psi(z)-2]f \tag{5.35}$$

for real functions $f(z)$, $z\in[0,1]$, with Dirichlet boundary conditions. With the normalization

$$1=\int_0^1 f(z)^2dz, \tag{5.36}$$

the variation of the ground state eigenvalue is

$$\frac{\delta\lambda^{(0)}}{\delta\psi(z)}=\left(\frac{\mathrm{Ra}}{4}\right)^{1/2}f(z)^2 \tag{5.37}$$

and so the Euler-Lagrange equations for the optimal ψ is

$$0=\frac{\delta}{\delta\psi(z)}\left[\frac{1}{2}\int_0^1\psi(z)^2dz+\alpha\int_0^1\psi(z)dz+\beta\lambda^{(0)}\right]$$

$$=\psi(z)+\alpha+\beta\left(\frac{\mathrm{Ra}}{4}\right)^{1/2}f(z)^2, \tag{5.38}$$

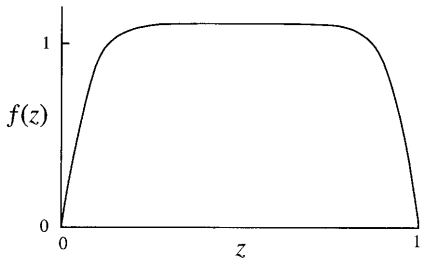

FIG. 7. Function $f(z)$, the solution of (5.41), for Ra=2000.

where α and β are Lagrange multipliers to be determined by the mean-zero condition (5.25) and by the condition that the ground state eigenvalue of (5.35) vanishes. Imposing (5.25), using the normalization (5.36), and integrating (5.38), we see that α and β are related by

$$0=\alpha+\beta\left(\frac{\mathrm{Ra}}{4}\right)^{1/2}. \tag{5.39}$$

Hence the Euler-Lagrange equation for $\psi(z)$ is

$$\psi(z)=\alpha f(z)^2-\alpha. \tag{5.40}$$

Inserting (5.40) into (5.35) and enforcing the $\lambda^{(0)}=0$ constraint, we arrive at the nonlinear Schrödinger (also known as Duffing) equation for f:

$$0=-D^2f+\left(\frac{\mathrm{Ra}}{4}\right)^{1/2}[\alpha f(z)^2-\alpha-2]f. \tag{5.41}$$

In the order we have formulated it here, the nonlinear boundary value problem in (5.41) is to be solved and then α is to be adjusted so that the normalization condition in (5.36) is enforced.

Equation (5.41) is relevant only for $\mathrm{Ra}\geqslant\pi^4\approx 97.4$; below that $\alpha=0$, $\psi\equiv 0$, the purely conductive background profile satisfies the spectral constraint, and Nu=1. Above $\mathrm{Ra}=\pi^4$ the exact solution of (5.41) is given in terms of Jacobi elliptic functions and this calculation has been fully carried out in the context of shear flow in Ref. [12]. The solution $f(z)$ is single signed and symmetric about the middle of the interval [0,1], as illustrated in Fig. 7. The large Rayleigh number asymptotic solution to (5.41), valid for $\mathrm{Ra}\to\infty$, is easier to manipulate analytically and that is how we will solve the problem here.

From the exact solution we observe that $\alpha\to\infty$ as $\mathrm{Ra}\to\infty$, so in the limit the D^2f term is negligible away from the boundaries $z=0$ and 1. Hence, in the middle of the interval $f(z)$ is approximately

$$f(z)\approx\left(\frac{\alpha+2}{\alpha}\right)^{1/2}. \tag{5.42}$$

Near the boundary at $z=0$, we change the independent variable to

$$x=Cz, \tag{5.43}$$

where

$$C=\left[\frac{\alpha+2}{2}\left(\frac{\mathrm{Ra}}{4}\right)^{1/2}\right]^{1/2}, \tag{5.44}$$

and the equation becomes

$$\frac{d^2f}{dx^2}=2\,\frac{\alpha}{\alpha+2}\,f(x)^3-2\,f(x), \tag{5.45}$$

with boundary conditions

$$f(0)=0, \quad f(x)\to\left(\frac{\alpha+2}{\alpha}\right)^{1/2} \quad \text{as} \quad x\to\infty. \tag{5.46}$$

The exact solution of (5.45) and (5.46) is

$$f(x)=\left(\frac{\alpha+2}{\alpha}\right)^{1/2}\tanh x, \tag{5.47}$$

which is seen to match up perfectly with the approximate solution away from the boundaries. This is the asymptotic form of the solution on the first half of the interval, and composite solutions, uniformly valid over the entire interval within exponentially small error of order e^{-C}, can be constructed either additively,

$$f(z)\approx\left(\frac{\alpha+2}{\alpha}\right)^{1/2}[\tanh Cz+\tanh C(1-z)-1], \tag{5.48}$$

or multiplicatively,

$$f(z)\approx\left(\frac{\alpha+2}{\alpha}\right)^{1/2}\tanh Cz\,\tanh C(1-z). \tag{5.49}$$

The value of α may now be determined by the normalization condition in (5.36), which is written on the half interval as

$$1=2\int_0^{1/2}f(z)^2dz=\frac{2}{C}\int_0^{C/2}f(x)^2dx$$

$$\approx\frac{2}{C}\,\frac{\alpha+2}{\alpha}\left[\frac{C}{2}-\tanh\frac{C}{2}\right]. \tag{5.50}$$

Neglecting exponentially small terms of order e^{-C}, this becomes

$$1\approx\frac{\alpha+2}{\alpha}\left[1-\frac{2}{C}\right], \tag{5.51}$$

yielding

$$\alpha+2\approx\left(\frac{\mathrm{Ra}}{16}\right)^{1/2}. \tag{5.52}$$

On the first half of the interval [0,1] the asymptotic form of the optimal function $\psi(z)$ is

$$\psi(z)=\alpha f(z)^2-\alpha\approx(\alpha+2)\tanh^2 Cz-\alpha. \tag{5.53}$$

Note then that

$$\psi(z)-2\approx(\alpha+2)[\tanh^2 Cz-1]<0, \tag{5.54}$$

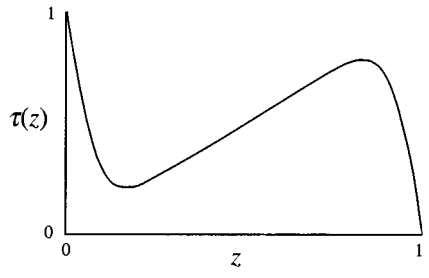

FIG. 8. Optimal background temperature profile of the modified variational problem, $\tau(z)$ resulting from (5.54), for Ra=2000. This profile is appropriately compared with the trial profile in Fig. 6, where the boundary layer in the profile was sketched with the thickness δ chosen according to (5.20) with Ra=2000.

so the functional K_ψ^- is manifestly positive. Hence the $\psi(z)$ that we have constructed here is indeed the true optimal solution. [That this procedure—constraining the variation only by the condition $K_\psi^+\geqslant 0$—yields the true optimal solution does not depend on the use of asymptotic methods; directly from (5.41) it is an easy exercise in one-degree-of-freedom Hamiltonian mechanics to show that the exact $\psi(z)<2$ pointwise.]

We are now in a position to evaluate the upper bound in (5.24). Recalling (5.40), we find

$$\begin{aligned}\mathrm{Nu}&\leqslant 1+\frac{1}{2}\int_0^1\psi(z)^2dz\\&=1+\frac{\alpha^2}{2}\int_0^1[f(z)^4-1]dz\\&=1+\frac{\alpha^2}{C}\int_0^{C/2}f(x)^4dx-\frac{\alpha^2}{2}\\&\approx 1+\frac{(\alpha+2)^2}{C}\int_0^{C/2}\tanh^4x\,dx-\frac{\alpha^2}{2}.\end{aligned} \tag{5.55}$$

Within exponentially small terms

$$\int_0^{C/2}\tanh^4x\,dx\approx\frac{C}{2}-\frac{4}{3}, \tag{5.56}$$

the upper bound reduces to

$$\mathrm{Nu}\leqslant 1+\frac{1}{2}\int_0^1\psi(z)^2dz\approx\tfrac{1}{6}\,\mathrm{Ra}^{1/2}-1, \tag{5.57}$$

a 33% reduction in the prefactor over the cruder estimate in (5.21). It is interesting to see that the structure of the optimal background temperature profile for this alternative formulation was qualitatively captured by the trial profile in (5.4), illustrated in Fig. 6. In Fig. 8 we plot the optimal profile for the alternative minimization problem; note the presence of the stable temperature stratification in the middle.

VI. OPTIMAL BOUNDS UTILIZING THE EULER-LAGRANGE EQUATIONS

The analysis in the preceding section was carried through without fully utilizing the incompressibility constraint on the velocity vector field. Incompressibility tends to lessen the normal component of the velocity near a no-slip surface because the vanishing tangential components force the normal derivative of the vertical component to vanish also. Hence it is expected that this feature may allow for a wider boundary layer while maintaining the spectral constraint, and hence a lower estimate on Nu. What we will show in this section is that the full optimal solution can take advantage of this effect and produce a lower scaling of the upper bound. Although we will not explicitly solve the optimal problem, we will deduce properties of the optimal profile from the Euler-Lagrange equations derived in Sec. IV. Here we study the case where the optimal profile lies on a codimension-1 portion of the marginally stable isospectral surface, so that the ground state is nondegenerate and the single wave number solution applies.

First we show that when there is no background flow field, the three-dimensional (3D) problem can be reduced to a 2D problem. Suppose we have the solution to the Fourier transformed eigenvalue problem (4.28)–(4.32) for $\lambda^{(0)}=0$:

$$0=(-D^2+k^2)u+ik_1p, \tag{6.1}$$

$$0=(-D^2+k^2)v+ik_2p, \tag{6.2}$$

$$0=(-D^2+k^2)w+Dp+\sqrt{\mathrm{Ra}}[\psi(z)-2]\theta, \tag{6.3}$$

$$0=ik_1u+ik_2v+Dw, \tag{6.4}$$

$$0=(-D^2+k^2)\theta+\sqrt{\mathrm{Ra}}[\psi(z)-2]w, \tag{6.5}$$

where $D=d/dz$ and ψ is related to w and θ by (4.35). The appearance of Ra has been ''symmetrized'' as in Sec. V. As outlined in Sec. IV, the wave vector $\mathbf{k}=(k_1,k_2)$ is presumed to have been chosen among the possibilities to maximize $\int\psi^2$. Then the change of dependent variables from u and v to $u\cos\varphi+v\sin\varphi$ and $-u\sin\varphi+v\cos\varphi$, where $\tan\varphi=k_2/k_1$, yields

$$0=(-D^2+k^2)u+ikp, \tag{6.6}$$

$$0=(-D^2+k^2)v, \tag{6.7}$$

$$0=(-D^2+k^2)w+Dp+\sqrt{\mathrm{Ra}}[\psi(z)-2]\theta, \tag{6.8}$$

$$0=iku+Dw, \tag{6.9}$$

$$0=(-D^2+k^2)\theta+\sqrt{\mathrm{Ra}}[\psi(z)-2]w, \tag{6.10}$$

where $k=|\mathbf{k}|=\sqrt{k_1^2+k_2^2}$, which does not vanish; there is no normalizable solution for $k=0$. Equation (6.7) is uncoupled and because the new u and v satisfy homogeneous Dirichlet boundary conditions at $z=0$ and 1, the solution for v is precisely $v(z)=0$. The remaining problem is just that derived from 2D convection in the x-z plane, with the length in the x direction an integer multiple of $2\pi/k$. It is possible that there are more than one vectors $\mathbf{k}$ for the optimal solution, in which case the resulting degeneracy of the ground state may be considered ''trivial'' in the sense that each yields parallel ψ and hence the same normal vector to the isospectral surface.

Eliminating u and p in (6.6)–(6.10), then, we obtain

$$0=k^{-2}(-D^2+k^2)^2w+\sqrt{\mathrm{Ra}}[\psi(z)-2]\theta, \tag{6.11}$$

$$0=(-D^2+k^2)\theta+\sqrt{\mathrm{Ra}}[\psi(z)-2]w. \tag{6.12}$$

When w and θ are the unique solution to (6.11) and (6.12), as we will consider for convenience, then without loss of generality they may both be taken to be real (if they were complex beyond a common phase factor, then the real and imaginary parts would each be independent solutions). The functional H_ψ for this solution vanishes:

$$0=\int_0^1\left\{\frac{1}{k^2}(D^2w)^2+2(Dw)^2+k^2w^2+(D\theta)^2+k^2\theta^2 + \sqrt{4\,\mathrm{Ra}}[\psi(z)-2]w\theta\right\}dz. \tag{6.13}$$

The optimal temperature gradient profile $\psi(z)$ is related to $w(z)$ and $\theta(z)$ as in (4.35),

$$\psi(z)=\alpha\left(w(z)\theta(z)-\int_0^1 w(z')\theta(z')dz'\right), \tag{6.14}$$

where the Lagrange multiplier α has been properly adjusted so that the solution exists and is normalized according to

$$1=\int_0^1\left\{\frac{1}{k^2}(Dw)^2+w^2+\theta^2\right\}dz. \tag{6.15}$$

Based on the experience gained from the analysis in Sec. V, we expect the solution $\psi(z)$ to be everywhere less than 2 with negative values in the boundary layers. Likewise, we expect the product $w(z)\theta(z)$ to be everywhere positive, analogous to the $f(z)^2$ from Sec. V; see Fig. 7. The Lagrange multiplier $\alpha>0$ [because of the parallel—not antiparallel—alignment of the vectors in Fig. 2(b)] and we expect it to scale as a positive power of Ra.

The upper bound on the heat transport may be expressed in terms of the eigenfunctions, using (6.13) and (6.14), as

$$\mathrm{Nu}-1\leqslant\frac{1}{2}\int_0^1\psi(z)^2dz$$
$$=\alpha\left(\int_0^1\left\{w\theta-\frac{1}{\sqrt{16\,\mathrm{Ra}}}\left[\frac{1}{k^2}(D^2w)^2+2(Dw)^2+k^2w^2+(D\theta)^2+k^2\theta^2\right]\right\}dz\right). \tag{6.16}$$

Because α is positive, this implies that the optimal solution satisfies

$$\int_0^1 w\theta\,dz>\frac{1}{\sqrt{16\,\mathrm{Ra}}}\int_0^1\left\{\frac{1}{k^2}(D^2w)^2+2(Dw)^2+k^2w^2+(D\theta)^2+k^2\theta^2\right\}dz. \tag{6.17}$$

Likewise, α may be expressed as a ratio of integrals of the solution

$$\alpha=2\frac{\int_0^1\left\{w\theta-\frac{1}{\sqrt{16\,\mathrm{Ra}}}\left[\frac{1}{k^2}(D^2w)^2+2(Dw)^2+k^2w^2+(D\theta)^2+k^2\theta^2\right]\right\}dz}{\int_0^1\left(w(z)\theta(z)-\int_0^1 w(z')\theta(z')dz'\right)^2dz} \tag{6.18}$$

and the bound on Nu is explicitly

$$\mathrm{Nu}-1\leqslant\frac{1}{2}\int_0^1\psi(z)^2dz=2\frac{\left(\int_0^1\left\{w\theta-\frac{1}{\sqrt{16\,\mathrm{Ra}}}\left[\frac{1}{k^2}(D^2w)^2+2(Dw)^2+k^2w^2+(D\theta)^2+k^2\theta^2\right]\right\}dz\right)^2}{\int_0^1\left(w(z)\theta(z)-\int_0^1 w(z')\theta(z')dz'\right)^2dz}. \tag{6.19}$$

At this point that we may establish a relationship between the optimal background field method and Howard's upper bound theory. Utilizing (6.17), we can throw away part of the numerator in (6.19) to derive an upper bound on the upper bound:

$$\mathrm{Nu}-1\leqslant\frac{1}{2}\int_0^1\psi(z)^2dz<2\frac{\left(\int_0^1 w\theta\,dz\right)\left(\int_0^1\left\{w\theta-\frac{1}{\sqrt{16\,\mathrm{Ra}}}\left[\frac{1}{k^2}(D^2w)^2+2(Dw)^2+k^2w^2+(D\theta)^2+k^2\theta^2\right]\right\}dz\right)}{\int_0^1\left(w(z)\theta(z)-\int_0^1 w(z')\theta(z')dz'\right)^2dz}. \tag{6.20}$$

The right-hand side above is precisely the expression for the heat transport at Rayleigh number 4 Ra utilizing the statistical stationarity closure and single mode hypothesis (which is apparently true for not-too-large Ra) made by Howard in [5]. Those hypotheses and that derivation, as well as the factor 4 rescaling of the Rayleigh number, is discussed in the Appendix, where a brief review of Howard's approach is presented. Howard's upper bound is sought as the largest possible value of the homogeneous functional of $w(z)$ and $\theta(z)$ in (6.20), maximized over functions satisfying the boundary conditions and $\int w\theta\,dz>0$. If we call the bound in (6.19) $B(\mathrm{Ra})$ and Howard's bound—the supremum of (6.20) at a quarter of the Rayleigh number—$B_H(\mathrm{Ra})$, then

$$\mathrm{Nu}-1\leqslant B(\mathrm{Ra})<B_H(4\,\mathrm{Ra}), \tag{6.21}$$

where the second inequality is strict (for nonstationary flows the first inequality is strict too). When the estimates scale with Ra, the bound derived by the optimal background field method is less than that of Howard's method modulo a prefactor. [Some of the prefactor discrepancy may be absorbed in the estimate going from (6.19) to (6.20).] The correspondence in (6.21) can in fact be made at an earlier stage in the analysis, prior to Fourier transforming, to elucidate the general connection between the estimates and this too is reserved for the Appendix. We may exploit this correspondence to utilize techniques from Howard's review [16(a)] to directly estimate the magnitude of the right-hand side in (6.19); in (6.19) w and θ are the solution of (6.11), (6.12), and (6.14), but an upper estimate may be established by bounding the largest value of the ratio of integrals over an enlarged function space.

First note that because the ratio is homogeneous in w and θ and $\int w\theta\,dz>0$, the normalization may be adjusted so that

$$1=\int_0^1 w(z)\theta(z)dz. \tag{6.22}$$

Then we seek the largest possible value of the ratio

$$\frac{\left(\int_0^1 \left\{ 1 - \frac{1}{\sqrt{16\,\mathrm{Ra}}} \left[\frac{1}{k^2} (D^2 w)^2 + 2(Dw)^2 + k^2 w^2 + (D\theta)^2 + k^2 \theta^2 \right] \right\} dz \right)^2}{\int_0^1 [w(z)\,\theta(z) - 1]^2 dz} \tag{6.23}$$

over functions $w(z)$ and $\theta(z)$ satisfying the normalization in (6.22), boundary conditions

$$w(0) = Dw(0) = \theta(0) = 0 = w(1) = Dw(1) = \theta(1), \tag{6.24}$$

and, from (6.17), the constraint

$$\int_0^1 \left\{ \frac{1}{k^2} (D^2 w)^2 + 2(Dw)^2 + k^2 w^2 + (D\theta)^2 + k^2 \theta^2 \right\} dz < \sqrt{16\,\mathrm{Ra}}. \tag{6.25}$$

We now use two of the technical results from Ref. [16(a)], which we will refer to as Howard's Lemma I and Howard's Lemma II. The proofs of these lemmas are sketched in the Appendix.

Howard's Lemma I. For functions $w(z)$ and $\theta(z)$ satisfying (6.22) and (6.24), there is a positive absolute constant $C_{\mathrm{I}} > 1.30$ such that

$$\int_0^1 [w(z)\,\theta(z) - 1]^2 dz \geqslant C_{\mathrm{I}} \left[\int_0^1 (D^2 w)^2 dz \right]^{-1/4} \left[\int_0^1 (D\theta)^2 dz \right]^{-1/4}. \tag{6.26}$$

Howard's Lemma II. For functions $w(z)$ and $\theta(z)$ satisfying (6.22) and (6.24), there is a positive absolute constant $C_{\mathrm{II}} > 2.20$ such that

$$\int_0^1 \left\{ \frac{1}{k^2} (D^2 w)^2 + 2(Dw)^2 + k^2 w^2 + (D\theta)^2 + k^2 \theta^2 \right\} dz \geqslant C_{\mathrm{II}} \left[\int_0^1 (D^2 w)^2 dz \right]^{1/3} \left[\int_0^1 (D\theta)^2 dz \right]^{1/3}, \tag{6.27}$$

uniformly in the wave number k.

These lemmas are utilized as follows. Howard's Lemma II asserts that in the regime where (6.25) holds, the numerator of (6.23) is

$$\left(\int_0^1 \left\{ 1 - \frac{1}{\sqrt{16\,\mathrm{Ra}}} \left[\frac{1}{k^2} (D^2 w)^2 + 2(Dw)^2 + k^2 w^2 + (D\theta)^2 + k^2 \theta^2 \right] \right\} dz \right)^2 \leqslant \left\{ 0{,}1 - \frac{C_{\mathrm{II}}}{\sqrt{16\,\mathrm{Ra}}} \left[\int_0^1 (D^2 w)^2 dz \right]^{1/3} \times \left[\int_0^1 (D\theta)^2 dz \right]^{1/3} \right\}^2. \tag{6.28}$$

Defining

$$X = \left[\int_0^1 (D^2 w)^2 dz \right]^{1/4} \left[\int_0^1 (D\theta)^2 dz \right]^{1/4} \tag{6.29}$$

and using Howard's Lemma I, (6.28) inserted into (6.19) yields

$$\mathrm{Nu} - 1 \leqslant \frac{1}{2} \int_0^1 \psi(z)^2 dz < \frac{2}{C_{\mathrm{I}}} X \left\{ 0{,}1 - \frac{C_{\mathrm{II}}}{\sqrt{16\,\mathrm{Ra}}} X^{4/3} \right\}^2. \tag{6.30}$$

Not knowing the value of X, we maximize over it to conclude that

$$\mathrm{Nu} - 1 \leqslant \frac{2}{C_{\mathrm{I}}} \frac{4}{7} \left(\frac{3}{7} \frac{\sqrt{16\,\mathrm{Ra}}}{C_{\mathrm{II}}} \right)^{3/4} \leqslant 0.257\ \mathrm{Ra}^{3/8}. \tag{6.31}$$

This bound is valid so long as the optimal background temperature profile has a nondegenerate ground state. We do not prove when this is the case; from the numerical analysis in Ref. [15] we observe that this is the case for $\mathrm{Ra} < 23\,300$. The optimal background profile has a degenerate ground state above $\mathrm{Ra} \approx 23\,300$ and the single wave number solutions are no longer relevant to the problem.

VII. DISCUSSION

The analysis presented in this paper establishes a fundamental and mathematically rigorous connection between the conditions for *stability* and the seemingly unrelated dynamics of unstable; unsteady convective motions including *turbulence*. This connection relies in an essential way on the relationship between the viscous Boussinesq dynamics and a related inviscid system (in the previous papers of this series the connection between Navier-Stokes dynamics and the inviscid Euler equations was exploited). The association of in-

viscid dynamics and turbulence is certainly not new, going back at least to the scaling ideas of Kolmogorov, nor is the use of marginal stability criteria to help explain characteristics of turbulent systems. But to the best of our knowledge the quantitative approach to turbulent dynamics in the Navier-Stokes and Boussinesq equations introduced and developed in this series of papers is the first to give a rigorous mathematical basis to this conception. While there remains much to understand regarding the interplay of viscous and inviscid properties of fluids and their motions, the techniques developed here offer an alternative view of this long-standing problem.

The next question is to determine the utility of this approach. The simplifications made in Sec. V allowed us to derive a rigorous analytic upper estimate of the form $\mathrm{Nu}\sim\mathrm{Ra}^{1/2}$, and using the optimal background field methods we derived an improved estimate of the form $\mathrm{Nu}\sim\mathrm{Ra}^{3/8}$ when the optimal background profile has a nondegenerate ground state (i.e., just one marginally stable mode), which is the case only for a bounded range in Ra ($\mathrm{Ra}\leqslant 23\,300$) [15]. (These are also the scalings found by Howard [5].) For higher Ra the optimal background profile has a degenerate ground state and it is likely that the degeneracy continues to increase so that more and more modes are marginally stable as the Rayleigh number is increased.

How good is the result of this analysis in comparison to theories of turbulence, to direct numerical simulations, and ultimately to experiments? And how practical will it be to fully exploit the methods proposed here? Can real improvements in the rigorous predictions be expected from further development of this mathematical procedure?

Experimental studies of thermal convection show different heat transport scaling behavior in different parameter regimes [17]. Not too far above the critical Rayleigh number where convection sets in, $\mathrm{Nu}\sim\mathrm{Ra}^{1/3}$ scaling is observed, and at higher Rayleigh numbers there is a crossover to $\mathrm{Nu}\sim\mathrm{Ra}^{2/7}$ scaling, a region of the dynamics known as ''hard turbulence'' [18]. Some recent experiments indicate the emergence of another boundary layer (shrinking $\sim\mathrm{Ra}^{-1/2}$) signaling an impending crossover to another region of $\mathrm{Nu}\sim\mathrm{Ra}^{1/2}$ scaling [19], which is the scaling we have proven here is an absolute upper bound.

The ''classical'' theory of convection explains the $\mathrm{Nu}\sim\mathrm{Ra}^{1/3}$ behavior by invoking a marginal stability condition on the conduction boundary layer [20]. The argument may be simply stated as follows: if a marginally stable thermal boundary layer of thickness δ (in dimensional units) forms, in which there is essentially no flow, then it must be that the Rayleigh number based on δ and half the temperature drop (the other half occurring across the other layer) is the critical Rayleigh number Ra_c. Then

$$\mathrm{Ra}_c=\frac{g\alpha(\delta T/2)\delta^3}{\nu\kappa}=\left(\frac{\delta}{h}\right)^3\frac{\mathrm{Ra}}{2}. \tag{7.1}$$

The Nusselt number scales as δ^{-1}, so this argument leads to the $\mathrm{Nu}\sim\mathrm{Ra}^{1/3}$ prediction. Compelling as this idea may be, it is far from a rigorous argument, e.g., Ra_c is ill defined due to the ambiguity of the boundary conditions to which it refers. The rigorous background field method presented here contains some strikingly similar features: if the entire profile (not just the boundary layer) is stable (in the sense of nonlinear energy stability) then the we may deduce an upper bound from it. The 3/8 scaling derived in Sec. VI is enticingly close to the classical 1/3 exponent, although its region of validity is relatively restricted.

A number of theories for the hard turbulent $\mathrm{Nu}\sim\mathrm{Ra}^{2/7}$ scaling have been developed in recent years [21], most of which directly exploit the observed large scale circulation, which both provides a stabilizing shear for the boundary layers and globally organizes the motion of smaller scale thermal plumes responsible for much of the heat transport. The implementation of a background flow profile together with the temperature profile is an obvious way to investigate this phenomenon in the context of the analysis presented in this paper, as well as to bring the Prandtl number into play regarding the bounds. These issues remain a challenge for the future.

The asymptotic $\mathrm{Nu}\sim\mathrm{Ra}^{1/2}$ scaling follows from Kraichnan's statistical turbulence theory closure model [22] [which additionally predicts logarithmic corrections to $\mathrm{Nu}\sim\mathrm{Ra}^{1/2}(\ln\mathrm{Ra})^{-3/2}$] as well as from Howard's upper bound theory [23]. So it appears that the rigorous bound resulting from the simplified calculation in Sec. V, $\mathrm{Nu}\sim\mathrm{Ra}^{1/2}$, is in accord with the asymptotic scaling expected on the basis of statistical turbulence theory, at least to within logarithms, and with the asymptotic scaling anticipated by experiments.

These results are all encouraging, and it is natural to investigate where there might be room for improvement in the estimates. The analyses in Secs. V and VI was simplified by excluding a background flow field. Because large scale shear is known to be an important component of the heat transfer in the hard turbulent regime, it will be interesting to see if the inclusion of a background flow improves the exponent in the bound. Because the elementary methods used in Sec. V will likely not reveal enhanced stability resulting from an imposed shear, the spectral constraint will almost surely have to be imposed exactly in order to see improvement. As previously noted, another interesting aspect of the problem that has been discarded in the no-background-flow case is the Prandtl number dependence of the heat transport. The Prandtl number enters this variational approach nontrivially only in the background shear contribution in the spectral constraint.

Ideally the variational problem for the optimal background profile laid out in Sec. IV will be solved exactly to yield the best estimates that this method has to offer. Although it is unlikely that exact analytical solutions will result, direct numerical solution of the nonlinear boundary value problem is possible [15] and those results will be discussed elsewhere. As far as analytical work is concerned, it is likely that matched asymptotic methods, such as those used to find f in Sec. V, may be fruitfully brought to bear. Given the similarity of the nonlinear Euler-Lagrange equation with those of Howard's theory, it is expected that some of his and Busse's asymptotic methods may be applied.

The two-dimensional version of the convection problem will be worthwhile to study in detail: direct numerical simulations in two dimensions display both the $\mathrm{Nu}\sim\mathrm{Ra}^{1/3}$ and $\mathrm{Ra}^{2/7}$ scalings [24,25], and special mathematical properties of 2D flows may be useful for the analysis [26]. Hence interesting behavior, with some of the characteristics of full 3D

turbulence, may reasonably be expected from this simplified problem. The Euler-Lagrange equations for the optimal background fields with a unique ground state in two dimensions are obtained from the results of Sec. IV by setting $v=0$ and $k_2=0$. Then the horizontal velocity component u and the pressure q may be eliminated, yielding a pair of coupled equations for $w(z)$ and $\zeta(z)$. The problem becomes

$$0=\sigma(-D^2+k^2)^2w+ikD[\phi(z)w]+ik\phi(z)Dw + \sigma\ \mathrm{Ra}k^2[\psi(z)-2]\zeta, \tag{7.2}$$

$$0=(-D^2+k^2)\zeta+[\psi(z)-2]w, \tag{7.3}$$

with boundary conditions w, Dw, and $\zeta=0$ for $z=0$ and 1. These equations are closed with the expressions for ϕ and ψ,

$$\phi(z)=\gamma\{i[Dw(z)^*w(z)-Dw(z)w(z)^*]-1\}, \tag{7.4}$$

$$\psi(z)=\gamma\{\zeta(z)^*w(z)+\zeta(z)w(z)^*-1\}. \tag{7.5}$$

In this formulation the Lagrange multiplier γ is adjusted so that the solutions satisfy

$$\int_0^1\phi(z)dz=0, \tag{7.6}$$

$$\int_0^1\psi(z)dz=0 \tag{7.7}$$

and the bound on the Nusselt number is

$$\mathrm{Nu}\leqslant 1+\frac{1}{2}\left(\frac{1}{\mathrm{Ra}}\int_0^1\phi(z)^2dz+\int_0^1\psi(z)^2dz\right), \tag{7.8}$$

where the wave number k is varied (over a discrete parameter set $\pm 2\pi n/L_x$ or over a continuous range for the most general situation) to maximize the right-hand side of (7.8). Further study of this particular problem (deriving solutions and/or estimates, determining the stability of the resulting background profiles, etc.) remains for the future.

It should be noted that the 3D problem with a background flow is *not* directly reducible to a 2D problem as is the case when ϕ is taken to be zero from the beginning. Nor, for that matter, do 3D shear flow problems, such as those studied in the first two papers in this series, Refs. [8, 12], reduce identically to 2D problems. It is interesting to note that for plane parallel background flow fields the 3D shear of problem of Ref. [8] maps onto the 2D convection problem *if* it is assumed that the most energy-unstable mode in a plane parallel shear flow is homogeneous in the streamwise direction. This is not known to be the case; this question also arises in the context of Howard's theory applied to shear flow problems and is discussed in that context in Busse's review, Ref. [16(b)].

Once the optimal profile has been obtained, whether for the 2D or the 3D problem, the self-adjoint eigenvalue problem associated with the spectral constraint leads to consideration of the complete set of eigenfunctions. These eigenfunctions will span the fluctuations about the background fields, and when the background profiles are optimal they provide a functional basis that is uniquely ''adapted'' to the turbulent flows, generated in a unique way from the fundamental equations of motion. It will be interesting to look at the structure of those flow fields with the hope that elements of the turbulent dynamics may be illuminated in these coordinates.

Those modal dynamical systems also offer a systematic approach to obtaining corrections to the best upper bounds produced by the optimal background fields. Indeed, recalling (3.15) we may assert the equality

$$2(\mathrm{Nu}-1)=\frac{1}{\mathrm{Ra}}\int_0^1\phi(z)^2dz+\int_0^1\psi(z)^2dz + \lim_{t\to\infty}\sup\left\langle -\frac{2}{A}H_{\phi,\psi}\{\mathbf{v},\theta\}\right\rangle_t. \tag{7.9}$$

Labeling the modes $\{\mathbf{v}_n,\theta_n\}$ of the spectral problem in the order of their magnitude $0=\lambda^{(0)}\leqslant\lambda^{(1)}\leqslant\lambda^{(2)}\leqslant\cdots$, we see that the general nonlinear solution for the fluctuation may be written

$$\begin{pmatrix}\mathbf{v}(\mathbf{x},t)\\ \theta(\mathbf{x},t)\end{pmatrix}=\sum_{n=0}^{\infty}a_n(t)\begin{pmatrix}\mathbf{v}_n(\mathbf{x})\\ \theta_n(\mathbf{x})\end{pmatrix}. \tag{7.10}$$

Then (7.9) may be reexpressed in terms of the time averaged squared modal amplitudes

$$2(\mathrm{Nu}-1)=\frac{1}{\mathrm{Ra}}\int_0^1\phi(z)^2dz+\int_0^1\psi(z)^2dz - \lim_{t\to\infty}\inf\frac{1}{A}\sum_{n=1}^{\infty}\lambda^{(n)}\langle|a_n(\ )|^2\rangle_t. \tag{7.11}$$

Including the contributions from the modal dynamics one by one produces a monotonically decreasing (and thus convergent) sequence of upper bounds. If the optimal background fields have a degenerate ground state, then modes beyond that number must be included before any decrease in the upper bound occurs.

Of course the exact modal dynamics is not available because the complete set of coupled amplitude evolution equations has the same overall complexity as the original partial differential equations. But we may truncate the amplitude evolution equations to obtain approximate dynamics for the modal amplitudes. These ''Galerkin truncations'' will lead to finite-dimensional dynamical systems models, akin to the re-

duced models derived from the proper orthogonal decomposition [27]. In fact, the modes derived from the spectral problem associated with energy stability analysis have previously been used for this purpose [28], the ultimate goal of this kind of theory being to develop control strategies for turbulent flows [29]. Further applications notwithstanding, the Galerkin truncations can provide a systematic—albeit not rigorously bounding—sequence of estimates when used in (7.11).

It is natural to be suspicious of the ability of any low-dimensional dynamical system to capture the essence of fully developed turbulent motions. The conventional picture for the universal energy distribution in homogeneous isotropic turbulence is the Kolmogorov spectrum $E(k)\sim\varepsilon^{2/3}k^{-5/3}$ up to the cutoff wavenumber scale $k_{\max}\sim\varepsilon^{1/4}$ (the inverse of the Kolmogorov length scale $\eta_K\sim\varepsilon^{-1/4}$) where exponential decay of the amplitudes sets in, so the energy dissipation rate $\sim k^2E(k)$ is dominated by contributions from modes at the small scales around $k_{\max}$. There are very many modes in the wave number shells about this scale and hence it appears unlikely that the energy dissipation can be quantitatively described by just a few modes and certainly not by large scale structures such as low-k Fourier modes or modes associated with a linearized evolution operator (e.g., Stokes modes). But there are two key points where this account may be questioned.

First, the picture coming from homogeneous isotropic theory does not necessarily apply the description of the situation for inhomogeneous anisotropic turbulence, such as wall-bounded flows, where definite small scale coherent structures can be identified as the dominant energy-containing modes, for example, via the proper orthogonal decomposition. The energy—and the energy dissipation and turbulent transport—is not democratically distributed over all the many small scale modes, but rather there are definite phase and amplitude relations that could conceivably result in a significant reduction in the number of independent dynamical degrees of freedom.

Second, modes produced by the spectral constraint associated with the optimal background flows will generally *not* be large scale Stokes-like modes, but rather small scale coherent structures. For the shear flow problem the lowest mode coming out of the spectral constraint are streamwise oriented wall bounded vortices whose diameters are on the scale of the boundary layer thickness [30], which at high Reynolds number is *smaller* than the bulk Kolmogorov scale η_K. The picture that emerges is one where the bulk dissipation is largely captured (and safely overestimated, apparently) by the contributions to the dissipation rate bounds from the background fields, while corrections due to the boundary layer structures are contained in the modal amplitude evolution taking place over the background fields. Whether or not this picture will survive quantitative tests remains to be seen.

Finally, we recall that the effective stability condition on the background fields in the variational problems developed in this series of papers is a stricter constraint than that which we really want to impose. The spectral constraint requires background profiles to be stable against all possible fluctuation fields, while in fact the basic calculation in (3.15) shows that all that is really required of background fields producing *exact* results (or upper bounds) is that they be marginally stable (or stable) ''on average'' in the sense that long time averages of $H_{\mathbf{U},\tau}$ vanish (or are positive). This is a weaker constraint than we have used in the analysis here, but it is awkward to impose because to exploit this relaxation requires some knowledge of the averaging process, i.e., some control of the temporal statistics of the solutions of the full nonlinear problem. As we have seen in the foregoing analysis, estimates of the magnitude of the global transport depend on the regularity of the allowed fluctuation fields in the boundary layers. The likelihood that an appropriate sense of ''averaged regularity'' of the fluctuations exceeds the uniform regularity utilized here opens the door to studies exploiting statistical features of turbulent solutions in an alternative way. That too will be left for future investigations.

In conclusion, the methods and results presented in this paper and in the previous papers in this series demonstrate the potential for rigorous analysis of the Navier-Stokes and related equations in problems of direct relevance to turbulence. Many mathematical challenges remain, but we are hopeful that continued development of these techniques will result in improved analytical estimates and eventually to more fundamental physical understanding of complex fluid dynamics.

ACKNOWLEDGMENTS

We thank F. Busse, S. Ghosal, S. Grossmann, P. Holmes, M. Holthaus, J. Hyman, R. Kerr, D. Lathrop, D. Lohse, A. Majda, D. Montgomery, D. Moore, I. Procaccia, E. Spiegel, K. Sreenivasan, P. Steen, A. Tilgner, N. Weiss, and J. Werne for helpful discussions, suggestions, and/or provoking comments. C.R.D. acknowledges the hospitality of the University of Chicago's Department of Mathematics, where this work was begun, as well as the Mathematical Sciences Research Institute at Berkeley, Bolyai College of Eötvös University in Budapest, Hungary, and the Antelope Retreat and Education Center, Savery, Wyoming, where much of this work was performed. P.C. and C.R.D. both acknowledge the extensive hospitality of the Isaac Newton Institute for Mathematical Sciences at the University of Cambridge, where this work was completed. The research reported here was supported in part by NSF and DOE.

APPENDIX: HOWARD'S THEORY AND HOWARD'S LEMMAS

Howard's upper bound theory, introduced in Ref. [5], is derived from the Boussinesq equations supplemented by a hypothesis of statistical stationarity, i.e., the technical assumption that horizontal averages, and thus also volume averages, are time independent. This is true for stationary flows, and for large aspect ratio systems it is a reasonable assumption; it could actually be valid in the limit of an infinite horizontal layer, but it has not been shown to follow from the equations of motion and it is likely not true in general in finite systems. In this section we will denote horizontal averages by $\langle\ \rangle$ and volume averages by $\langle\langle\ \rangle\rangle$, and we will use the notation $\mathbf{u}=(u,v,w)$.

The theory proceeds from the Boussinesq equations

$$\frac{\partial\mathbf{u}}{\partial t}+\mathbf{u}\cdot\boldsymbol{\nabla}\mathbf{u}+\boldsymbol{\nabla}p=\sigma\Delta\mathbf{u}+\sigma\ \mathrm{Ra}\mathbf{k}T, \tag{A1}$$

$$\boldsymbol{\nabla}\cdot\mathbf{u}=0, \tag{A2}$$

$$\frac{\partial T}{\partial t}+\mathbf{u}\cdot\boldsymbol{\nabla}T=\Delta T \tag{A3}$$

by deriving the relations analagous to (1.10), (1.13), and (1.15) between the Nusselt number

$$\mathrm{Nu}=1+\langle\langle wT\rangle\rangle, \tag{A4}$$

and the dissipation rates. Invoking the statistical stationarity hypothesis, standard calculations yield

$$\mathrm{Nu}=\langle\langle|\boldsymbol{\nabla}T|^2\rangle\rangle \tag{A5}$$

and

$$\mathrm{Ra}(\mathrm{Nu}-1)=\langle\langle|\boldsymbol{\nabla}\mathbf{u}|^2\rangle\rangle. \tag{A6}$$

The temperature is decomposed into a horizontal average and a fluctuation

$$T(\mathbf{x},t)=\langle T\rangle(z)+\theta(\mathbf{x},t). \tag{A7}$$

The mean temperature profile $\langle T\rangle(z)$ satisfies the boundary conditions on the top and bottom, $\langle T\rangle(0)=1$ and $\langle T\rangle(1)=0$, and so θ vanishes there. It is easy to see that $\mathrm{Nu}-1=\langle\langle w\theta\rangle\rangle$ using incompressibility. The horizontal average of the temperature evolution equation (A3) combined with the boundary conditions gives

$$\langle w\theta\rangle-\langle\langle w\theta\rangle\rangle=\frac{d\langle T\rangle}{dz}+1, \tag{A8}$$

which, when inserted into (A5) to eliminate the mean, yields

$$\mathrm{Nu}-1=\langle\langle|\boldsymbol{\nabla}\theta|^2\rangle\rangle+\langle\langle(\langle w\theta\rangle-\langle\langle w\theta\rangle\rangle)^2\rangle\rangle. \tag{A9}$$

In essence, Howard's upper bound theory consists of maximizing $\mathrm{Nu}-1=\langle\langle w\theta\rangle\rangle$ subject to the constraints in (A6) and (A9). It is convenient to cast the variational problem in the form of a nonlinear Dirichlet ratio, as follows.

Adding together the expressions for $\mathrm{Nu}-1$ from (A6) and (A9) gives

$$2(\mathrm{Nu}-1)=2\langle\langle w\theta\rangle\rangle=\frac{1}{\mathrm{Ra}}\langle\langle|\boldsymbol{\nabla}\mathbf{u}|^2\rangle\rangle+\langle\langle|\boldsymbol{\nabla}\theta|^2\rangle\rangle+\langle\langle(\langle w\theta\rangle-\langle\langle w\theta\rangle\rangle)^2\rangle\rangle, \tag{A10}$$

and rearranging slightly produces an expression for the identity:

$$1=\frac{2\langle\langle w\theta\rangle\rangle-\left[\frac{1}{\mathrm{Ra}}\langle\langle|\boldsymbol{\nabla}\mathbf{u}|^2\rangle\rangle+\langle\langle|\boldsymbol{\nabla}\theta|^2\rangle\rangle\right]}{\langle\langle(\langle w\theta\rangle-\langle\langle w\theta\rangle\rangle)^2\rangle\rangle}. \tag{A11}$$

Finally, multiplying by $\mathrm{Nu}-1=\langle\langle w\theta\rangle\rangle$ gives

$$\mathrm{Nu}-1=2\,\frac{\langle\langle w\theta\rangle\rangle^2-\langle\langle w\theta\rangle\rangle\left[\frac{1}{2\,\mathrm{Ra}}\langle\langle|\boldsymbol{\nabla}\mathbf{u}|^2\rangle\rangle+\frac{1}{2}\langle\langle|\boldsymbol{\nabla}\theta|^2\rangle\rangle\right]}{\langle\langle(\langle w\theta\rangle-\langle\langle w\theta\rangle\rangle)^2\rangle\rangle}. \tag{A12}$$

Substituting $\mathbf{u}'=\mathbf{u}/\sqrt{\mathrm{Ra}}$ in place of $\mathbf{u}$ and dropping the prime, (A12) becomes

$$\mathrm{Nu}-1=2\,\frac{\langle\langle w\theta\rangle\rangle^2-\langle\langle w\theta\rangle\rangle\,\frac{1}{\sqrt{4\,\mathrm{Ra}}}\left[\langle\langle|\boldsymbol{\nabla}\mathbf{u}|^2\rangle\rangle+\langle\langle|\boldsymbol{\nabla}\theta|^2\rangle\rangle\right]}{\langle\langle(\langle w\theta\rangle-\langle\langle w\theta\rangle\rangle)^2\rangle\rangle}. \tag{A13}$$

Howard's upper bound, denoted $B_H(\mathrm{Ra})$, is sought as the largest possible value of the homogeneous ratio in (A13),

$$\mathrm{Nu}-1\leq B_H(\mathrm{Ra})=\sup 2\,\frac{\langle\langle w\theta\rangle\rangle^2-\langle\langle w\theta\rangle\rangle\,\frac{1}{\sqrt{4\,\mathrm{Ra}}}\left[\langle\langle|\boldsymbol{\nabla}\mathbf{u}|^2\rangle\rangle+\langle\langle|\boldsymbol{\nabla}\theta|^2\rangle\rangle\right]}{\langle\langle(\langle w\theta\rangle-\langle\langle w\theta\rangle\rangle)^2\rangle\rangle}, \tag{A14}$$

maximized over divergence-free vector fields $\mathbf{u}$ and functions θ satisfying Dirichlet boundary conditions at $z=0$ and 1. This set contains all possible solutions of the original Boussinesq equations, so given the statistical stationarity hypothesis, the resulting upper bound applies to the time averaged heat transport.

It is straightforward to check that the Euler-Lagrange equations for Howard's variational problem (A14) coincide in form with those for the optimal background field, but with different Lagrange multipliers in different places enforcing different constraints. This strikes us as a somewhat amazing correspondence: the bound from the *optimal* background profile satisfies a relation that is similar in form to the foundation of Howard's variational problem, i.e., a statistical power balance. The correspondence for this problem is also intriguing because of other fundamental differences in the

approaches: the background field formalism allows for symmetry breaking flow fields—the implications of which have not been fully explored in this paper—whereas the statistical stationarity hypothesis seems to inextricably force the symmetry of the geometry into Howard's variational problem. Moreover, it is not clear what would take the place of the horizontal averaging procedure in case the problem is posed in geometries without obvious symmetries; these are also nontrivial problems for the background field method because of the need there to identify the appropriate space of stable background flows and temperature fields.

The expression in (A13) is remarkably similar to the optimal upper bound $B(\mathrm{Ra})$ derived from the background field method; in the present notation (6.19) is

$$\mathrm{Nu}-1\leqslant\frac{1}{2}\int_0^1\psi(z)^2dz=B(\mathrm{Ra})$$
$$=2\frac{\left(\langle\langle w\theta\rangle\rangle-\frac{1}{\sqrt{16\,\mathrm{Ra}}}\left[\langle\langle|\nabla\mathbf{u}|^2\rangle\rangle+\langle\langle|\nabla\theta|^2\rangle\rangle\right]\right)^2}{\langle\langle(\langle w\theta\rangle-\langle\langle w\theta\rangle\rangle)^2\rangle\rangle},\tag{A14$'$}$$

where the pair $(\mathbf{u},\theta)$ is the solution to (6.11) and (6.12). Because the Lagrange multiplier $\alpha>0$, the numerator above is the square of a positive number and an expression such as that in (A.14) is recovered as a strict upper estimate and the connection with Howard's bound is established:

$$B(\mathrm{Ra})<2\frac{\langle\langle w\theta\rangle\rangle^2-\langle\langle w\theta\rangle\rangle\frac{1}{\sqrt{16\,\mathrm{Ra}}}\left[\langle\langle|\nabla\mathbf{u}|^2\rangle\rangle+\langle\langle|\nabla\theta|^2\rangle\rangle\right]}{\langle\langle(\langle w\theta\rangle-\langle\langle w\theta\rangle\rangle)^2\rangle\rangle}\leqslant B_H(4\,\mathrm{Ra}).\tag{A15}$$

For the estimate in Sec. VI, however, we did not attempt a solution of the Euler-Lagrange equations. Rather, in the spirit of Howard's theory, we sought the largest possible value of the ratio in (A14$'$) over a set of functions that contains the solution.

We now turn to the proofs of the two technical lemmas from Howard's analysis in Ref. [16](a) that were used in Sec. VI to bound the ratio. As will be seen, the analysis is very similar in nature to that used to derive the estimates in Sec. V.

Howard's Lemma I. For functions $w(z)$ and $\theta(z)$ satisfying boundary conditions $w(0)=Dw(0)=\theta(0)=0=w(1)=Dw(1)=\theta(1)$ and $\int w\theta=1$, there is a positive constant C_{I} such that

$$\int_0^1[w(z)\theta(z)-1]^2dz\geqslant C_{\mathrm{I}}\left[\int_0^1(D^2w)^2dz\right]^{-1/4}\times\left[\int_0^1(D\theta)^2dz\right]^{-1/4}.\tag{A16}$$

Proof. First note that in light of the boundary conditions at $z=0$, using the fundamental theorem of calculus and the Cauchy-Schwarz inequality,

$$|\theta(z)|=\left|\int_0^z D\theta(z')dz'\right|\leqslant\sqrt{z}\left[\int_0^1(D\theta)^2dz\right]^{1/2}.\tag{A17}$$

Similarly,

$$|w(z)|=\left|\int_0^z dz'\int_0^{z'}dz''D^2w(z'')\right|\leqslant\tfrac{2}{3}z^{3/2}\left[\int_0^1(D^2w)^2dz\right]^{1/2}.\tag{A18}$$

Define the ''boundary layer thickness'' δ according to

$$\frac{1}{\delta^2}=\frac{2}{3}\left[\int_0^1(D\theta)^2dz\right]^{1/2}\left[\int_0^1(D^2w)^2dz\right]^{1/2}.\tag{A19}$$

Note that $\delta<\frac{1}{2}$; indeed, the normalization $\int w\theta=1$ together with the Poincaré inequality implies

$$1=\int_0^1w(z)\theta(z)dz\leqslant\pi^3\left[\int_0^1(D^2w)^2dz\right]^{1/2}\left[\int_0^1(D\theta)^2dz\right]^{1/2}$$
$$=\frac{3\pi^3}{2\delta^2}.\tag{A20}$$

Then the integrand on the left-hand side of (A16) is bounded from below pointwise on $[0,\delta]$ as

$$[1-w(z)\theta(z)]^2\geqslant\left(1-\frac{z^2}{\delta^2}\right)^2\tag{A21}$$

and similarly from the other end of the interval with $z\to1-z$. Then,

$$\int_0^1[w(z)\theta(z)-1]^2dz$$
$$\geqslant\int_0^\delta\left(1-\frac{z^2}{\delta^2}\right)^2dz+\int_{1-\delta}^1\left(1-\frac{(1-z)^2}{\delta^2}\right)^2dz$$
$$\geqslant2\delta\int_0^1(1-x^2)^2dx$$
$$=\tfrac{16}{15}\delta=\tfrac{16}{15}(\tfrac{3}{2})^{1/2}\left[\int_0^1(D\theta)^2dz\right]^{-1/4}\left[\int_0^1(D^2w)^2dz\right]^{-1/4}.\tag{A22}$$

Hence the lemma is proved and $C_{\mathrm{I}}\approx1.31$ is an estimate for the constant.

Howard's Lemma II. For functions $w(z)$ and $\theta(z)$ satisfying $w(0)=Dw(0)=\theta(0)=0=w(1)=Dw(1)=\theta(1)$ and $\int w\theta=1$, there is a positive constant $C_{\rm II}$ such that

$$M\equiv\int_0^1\left\{\frac{1}{k^2}(D^2w)^2+2(Dw)^2+k^2w^2+(D\theta)^2+k^2\theta^2\right\}dz \geq C_{\rm II}\left[\int_0^1(D^2w)^2dz\right]^{1/3}\left[\int_0^1(D\theta)^{22}dz\right]^{1/3}, \tag{A23}$$

uniformly in the wave number k.

Proof. First note that from the normalization,

$$1=\int_0^1 w(z)\theta(z)dz\leq\left(\int_0^1 w(z)^2dz\right)^{1/2}\left(\int_0^1\theta(z)^2dz\right)^{1/2}, \tag{A24}$$

so

$$M\geq\frac{1}{k^2}\int_0^1(D^2w)^2dz+k^2\left(\int_0^1 w^2dz+\frac{1}{\int w^2dz}\right)+\int_0^1(D\theta)^2dz. \tag{A25}$$

Then note that

$$\int_0^1 w^2dz+\frac{1}{\int w^2dz}\geq 2, \tag{A26}$$

so

$$M\geq\frac{1}{k^2}\int_0^1(D^2w)^2dz+2k^2+\int_0^1(D\theta)^2dz. \tag{A27}$$

Minimizing over k^2, we deduce

$$M\geq 2\sqrt{2}\left[\int_0^1(D^2w)^2dz\right]^{1/2}+\int_0^1(D\theta)^2dz. \tag{A28}$$

Using Hölder's inequality ($ab\leq a^p/p+b^q/q$ for $1=1/p+1/q$) with $p=3/2$ and $q=3$ and appropriately chosen a and b, we see that

$$M\geq(\tfrac{32}{3})^{1/3}\left[\int_0^1(D^2w)^2dz\right]^{1/3}\left[\int_0^1(D\theta)^2dz\right]^{1/3}. \tag{A29}$$

This both establishes the lemma and provides a numerical estimate $C_{\rm II}\approx 2.20$ for the constant.

[1] H. Tennekes and J. L. Lumley, *A First Course in Turbulence* (MIT Press, Cambridge, MA, 1972).

[2] R. Temam, *Navier-Stokes Equations and Nonlinear Functional Analysis* (SIAM, Philadelphia, 1983); P. Constantin and C. Foias, *Navier-Stokes Equations* (University of Chicago Press, Chicago, 1988); C. R. Doering and J. D. Gibbon, *Applied Analysis of the Navier-Stokes Equations*, Cambridge Texts in Applied Mathematics (Cambridge University Press, Cambridge, England, 1995).

[3] E. Hopf, Math. Ann. **117**, 764 (1941).

[4] D. D. Joseph, *Stability of Fluid Motions* (Springer, New York, 1976); B. Straughan, *The Energy Method, Stability and Nonlinear Convection* (Springer-Verlag, Berlin, 1992).

[5] L. N. Howard, J. Fluid Mech. **17**, 405 (1963).

[6] F. H. Busse, J. Fluid Mech. **37**, 457 (1969).

[7] C. R. Doering and P. Constantin, Phys. Rev. Lett. **69**, 1648 (1992); **69**, 3000(E) (1992); for a review, see B. Bayley, Phys. World **5**, 18 (1992).

[8] C. R. Doering and P. Constantin, Phys. Rev. E **49**, 4087 (1994).

[9] D. P. Lathrop, J. Feinberg, and H. L. Swinney, Phys. Rev. Lett. **68**, 1515 (1992); Phys. Rev. A **46**, 6390 (1992).

[10] C. Marchioro, Physica D **74**, 395 (1994).

[11] T. Gebhardt, S. Grossmann, M. Holthaus, and M. Löhden, Phys. Rev. E **51**, 360 (1995).

[12] P. Constantin and C. R. Doering, Phys. Rev. E **51**, 3192 (1995).

[13] S. Chandrasekhar, *Hydrodynamic and Hydromagnetic Stability* (Dover, New York, 1961); P. Drazin and W. Reid, *Hydrodynamic Stability* (Cambridge University Press, Cambridge, England, 1981).

[14] P. Constantin and C. R. Doering, Physica D **82**, 221 (1995).

[15] C. R. Doering and J. M. Hyman (unpublished).

[16] The theory introduced in Ref. [5] enjoyed well over a decade's development and application to a variety of problems. For comprehensive reviews see (a) L. N. Howard, Annu. Rev. Fluid Mech. **4**, 473 (1972); (b) F. H. Busse, Adv. Appl. Mech. **18**, 77 (1978). See also the many examples and applications in Joseph's book, Ref. [4].

[17] For a review, see E. Siggia, Annu. Rev. Fluid Mech. **26**, 137 (1994).

[18] F. Heslot, B. Castaing, and A. Libchaber, Phys. Rev. A **36**, 5870 (1987).

[19] A. Belmonte, A. Tilgner, and A. Libchaber, Phys. Rev. E **50**, 269 (1994).

[20] W. V. R. Malkus and G. Veronis, J. Fluid Mech. **4**, 225 (1958).

[21] B. Castaing, G. Gunaratne, F. Heslot, L. P. Kadanoff, A. Libchaber, S. Thomae, X.-Z. Wu, S. Zaleski, and G. Zanetti, J. Fluid Mech. **204**, 1 (1989); Z.-S. She, Phys. Fluids A **1**, 911 (1989); B. I. Shraiman and E. D. Siggia, Phys. Rev. A **42**, 3650 (1990); V. Yakhot, Phys. Rev. Lett. **69**, 769 (1992); J. Werne, Phys. Rev. E **49**, 4072 (1994).

[22] R. Kraichnan, Phys. Fluids **5**, 1374 (1962).

[23] Busse implemented the divergence-free condition in Howard's method using asymptotic methods and although the scaling remained the same, the prefactor was improved to $\sqrt{\mathrm{Ra}/1035}$; see Ref. [6]. The classical scaling $\mathrm{Nu}\sim\mathrm{Ra}^{1/3}$ has been deduced from Howard's method in the infinite Prandtl number limit where the velocity field is slaved to the temperature field's evolution; see S.-K. Chan, Stud. Appl. Math. **50**, 13 (1971).

[24] E. E. DeLuca, J. Werne, and R. Rosner, Phys. Rev. Lett. **64**, 2370 (1990); J. Werne, E. E. DeLuca, R. Rosner, and F. Cattaneo, *ibid.* **67**, 3519 (1991); J. Werne, Phys. Rev. E **48**, 1020 (1993).

[25] The scaling $Nu \sim Ra^{0.365}$ has been observed in 2D simulations, very close to the 3/8 exponent, but with stress-free boundary conditions (i.e., $\partial v_x/\partial z = 0 = \partial v_y/\partial z$, rather than the $v_x = 0 = v_y$ no-slip conditions) on the rigid surfaces; see D. R. Moore and N. O. Weiss, J. Fluid Mech. **58**, 289 (1973). The analysis in this paper does not directly apply to stress-free boundaries and it is not unexpected for the heat transport to be higher in that case than with sticky boundaries.

[26] See, for example, I. Herron, Stud. Appl. Math. **85**, 269 (1991).

[27] N. Aubry, P. Holmes, J. L. Lumley, and E. Stone, J. Fluid Mech. **192**, 115 (1988).

[28] A. C. Poje and J. L. Lumley, J. Fluid Mech. **285**, 349 (1995).

[29] B. D. Coller, P. Holmes, and J. L. Lumley, Appl. Mech. Rev. **47**, S139 (1994).

[30] M. A. Orwoll, Ph.D. thesis, Clarkson University, 1994 (unpublished).